REPUBLIC OF TÜRKİYE

ALTINBAŞ UNIVERSITY

Institute of Graduate Studies

Civil Engineering

STUDY THE IMPACT OF OPENING ON THE HYSTERETIC RESPONSE OF SHEAR WALL

Zeanalabdeen GHURAIBAW

Master's Thesis

Supervisor

Assoc. Prof. Dr. Sepanta NAİMİ

Istanbul, 2023

STUDY THE IMPACT OF OPENING ON THE HYSTERETIC RESPONSE OF SHEAR WALL

Zeanalabdeen GHURAIBAW

Civil Engineering

Master's Thesis

ALTINBAŞ UNIVERSITY

2023

The thesis titled STUDY THE IMPACT OF OPENING ON THE HYSTERETIC RESPONSE OF SHEAR WALL prepared by ZEANALABDEEN GHURAIBAW and submitted on 14/04/2023 has been **accepted unanimously** for the degree of Master of Science in Civil Engineering

____
Assoc. Prof. Dr. Sepanta NAİMİ
Supervisor

Thesis Defense Committee Members:

Assoc. Prof. Dr. Sepanta NAİMİ	Department of Civil Engineering, Altınbaş University	_______________
Asst. Prof. Dr. Mohsen SEYEDİ	Department of Civil Engineering, Altınbaş University	_______________
Assoc. Prof. Dr. İsmail Cengiz YILMAZ	Department of Engineering and Architecture, Istanbul Arel University	_______________

I hereby declare that this thesis meets all format and submission requirements of a Master's thesis.

Submission date of the thesis to Institute of Graduate Studies: ___/___/___

I hereby declare that all information/data presented in this graduation project has been obtained in full accordance with academic rules and ethical conduct. I also declare all unoriginal materials and conclusions have been cited in the text and all references mentioned in the Reference List have been cited in the text, and vice versa as required by the abovementioned rules and conduct.

Zeanalabdeen GHURAIBAW

Signature

DEDICATION

I want to express my gratitude to my parents, who have always been there for me and done the most for me. I couldn't have finished my task without their constant encouragement and positive reinforcement. It would be inexcusable of me not to explain to my closest friends and family how much I value their understanding and encouragement. Whether I was pleased or sad, they were there to cheer me up and tell me I could do anything. Lastly, I'd like to express my gratitude to everyone who helped keep me from feeling alone and isolated during my time here.

PREFACE

Before anything else, I'd like to give thanks to God for blessing me with the perseverance and fortitude to succeed in my endeavour.

Thereafter, I'd want to express my deepest gratitude to my supervisor, for his unending guidance and support during the duration of the project, as well as for his patience, inspiration, and wealth of knowledge. Under his guidance, I've been able to become more independent as I've conducted research for my thesis. I hope the best for him in anything he does. I'd also like to express my gratitude to the other members of my thesis committee for their insightful criticism and assistance.

Furthermore, I'd like to express my gratitude to everyone who has ever believed in me or supported me as I worked toward my goal of earning a college degree.

One final thing I'd want to say is how grateful I am to my fellow master’s students and to my co-workers for their moral and emotional support during my thesis writing and research process.

ABSTRACT

STUDY THE IMPACT OF OPENING ON THE HYSTERETIC RESPONSE OF SHEAR WALL

GHURAIBAW, Zeanalabdeen

M.Sc., Civil Engineering, Altınbaş University,

Supervisor: Assoc. Prof. Dr. Sepanta NAİMİ

Date: April / 2023

Pages: 85

Structures often use shear walls made of reinforced concrete to stop things from moving sideways. Depending on where they are and what they do, the walls of the building can be flat, connected, or core walls. Shear wall systems work best for low-rise buildings with up to 20 stories (Bungle). They use more material than walls that don't bend and frames that don't bend. Shear wall solutions shouldn't be used in buildings that have a lot of glass or walls that are see-through. Because the fundamental periods are short and the drift between floors is limited, these systems are good for low and mid-rise buildings because they are stable and resistive. Shear wall systems can still withstand earthquake loads even though they have a higher structural base shear force than other resistant systems. Shear walls that are joined together and held up by beams can span larger gaps. They can be as strong as a stiff frame or as strong as a whole wall. This study looks at the relationship between the length of the construction and the size of the shear wall aperture. figuring out the largest ratios of slot length to sidewall length that can be ignored by modelling. If designers know the smallest opening ratio at which a solid wall becomes a frame, they can make their models safe and easy to use. To figure out how long a shear wall structure will last, the ASCE7-16 code formula and the results of finite element analysis are compared. Apertures can change the basic period and sideways movement of shear wall systems. Modeling involves two stages. This level looks at how these gaps affect how common structures are shown in 3D. A formula for growth over time was also brought up. The main results and conclusions of the study come after this introduction.

Keywords: Shear Wall, ABAQUS, Finite Elements, Seismic Performance, Structural Stability.

TABLE OF CONTENTS

Pages

LIST OF TABLES

Pages

LIST OF FIGURES

Pages

ABBREVIATIONS

ABAQUS	:	Finite element program
ACI	:	American Concrete Institute
AISC	:	American Institute of Steel Construction
ASCE	:	American Society of Civil Engineers
BFRP	:	Basalt Fibre Reinforced Polymer
CDP	:	Concrete Damaged Plasticity model
CFD	:	Computational Fluid Dynamics
DIC	:	Digital Image Correlation
DOF	:	Degrees of Freedom
EBF	:	Eccentric Braced Frame
EXP	:	Experimental
FEA	:	Finite Element Analysis
FEMA	:	Federal Emergency Management Agency
FP	:	Fundamental Period
FRP	:	Fibre Reinforced Polymer
IBC	:	International Building Code
IDA	:	Incremental Dynamic Analysis
ISO	:	International Organization for Standardization
LRFD	:	Load and Resistance Factor Design
LVDT	:	Linear Variable Displacement Transducer

MCE	:	Maximum Considered Earthquake
MCFT	:	Modified Compression Field Theory
NEHRP	:	National Earthquake Hazards Reduction Program
PSD	:	Power Spectral Density
RCC	:	Reinforced Cement Concrete
SD	:	Standard Deviation
SFRC	:	Steel Fibre-Reinforced Concrete
SW	:	Shear Wall
SWS	:	Shear Wall Structure

1. INTRODUCTION

1.1 INTRODUCTION

This chapter will begin with an introduction that includes a brief discussion of a shear wall structure, followed by an analysis of its challenges and goals. Buildings, in general, need to be strong to sustain tremors caused by earthquakes as well as other lateral loads. Increasing the capacity for stiffness can be accomplished by the utilization of several lateral bracing methods, one of which is the shear wall system.

1.2 THE COMPONENTS AND SYSTEMS OF THE SHEAR WALLS

Reinforced concrete shear walls are the most often used lateral-force-resisting structural elements. There are a variety of ways to build these walls, including core walls, linked walls, and planar walls, depending on the location and function of the walls. In low-rise and medium sized structures with a maximum of 20 stories, shear wall systems are the best option for utilization (Bungle). Because of the substantial use of materials in this system in compared to the use of materials in other lateral bracing methods, such as moment resisting frames, high-rise buildings do not choose this type of bracing. Shear wall systems are not suggested for use in open-space buildings or on exterior walls that are glazed because of their architectural functions. Low- to mid-rise structures can benefit from these systems because of their low drift between floors and short undamped fundamental time. Because of these elements, the buildings are more stable. However, despite the fact that shear wall systems often have higher internal base shear forces, they are able to endure earthquakes' tremendous forces.

Patterns of windows and doors in walls are necessary for architectural objectives, as was previously stated. When large apertures are involved, the walls are referred to as coupled shear walls because beams join them. As a result, the wall's stiffness changes from that of a solid wall to that of an extensible frame as a result of the apertures. This is a shift from a rigid wall to a more malleable frame.

1.2.1 Fundamental Period

Free vibration occurs in a structure whenever it is subjected to a lateral load, such as when it is shaken by an earthquake. This causes the structure to oscillate back and forth. The amount of time necessary to finish one cycle of free vibration is referred to as the natural period, and the inverse of this term is known as the natural frequency. The structure's fundamental period is a crucial attribute to take into consideration while characterizing the dynamic behaviour of the structure. There are three different approaches that can be utilized in order to ascertain a structure's natural period: theoretical models, numerical models, and empirical formulas.

Empirical formulas are the first thing that are used when designing a new structure because it is impossible to compute the properties of a building that has not yet been designed; the only properties that can be calculated at this point are those related to the materials that are used, the lateral bracing system (reinforced concrete shear walls), the steel moment resisting frames, and the dual system. Empirical formulas are used because it is impossible to compute the properties of a building that has not yet been designed. After the early stage of design, it is usual practice to use theoretical and numerical models because these models require more information in the computations.

Models with one degree of freedom are the most straightforward representations of the applicable theoretical technique. Calculating the natural period of this model with no damping applied is possible using the following formula:

$$T = 2\pi\sqrt{\frac{m}{K}} \tag{1-1}$$

Where:

m is the structure's mass.

k: The structure's stiffness.

Many methods for estimating the basic period have been devised in theoretical models, including Dunkerley's method (Bishop and Johnson) and Rayleigh's method. The natural period of the system can be calculated using the lumped weights distribution model in

Rayleigh's approach for rapid estimation. This method is based on the conservation of energy principle, which dictates that the maximum velocity must equal the full possible energy in the absence of damping. The approach is applicable to systems with multiple degrees of freedom. This method is used as a rational way in many codes, and the period is calculated using the equation:

$$T = 2\pi\sqrt{\sum_{i=1}^{n}\omega i\delta_i^2 \div (g\sum_{i=1}^{n} fi\delta i)} \tag{1-2}$$

Where:

fi: Lateral force at floor level.

δi: Elastic deflection caused by lateral force at floor level i.

g: Gravitational acceleration

wi: Weight at the first-floor level.

1.3 SHEAR WALL SYSTEM WITH LATERAL LOAD RESISTANT DESIGN

1.3.1 Important Design Considerations

Maximum yield values from the American Society of Civil Engineers (ASCE) and the National Design Specification (NDS) are utilized in the computation of the design loads that are applied to a conventional building a shear wall using a timber frame. Once the values were assigned have been figured out, the shear wall styling can be completed by making sure the design parts are in the right proportions and are connected in the right way. The process of design comprises activities such as calculating the thickness of the sheathing, nailing the shear walls, designing the chords and collectors, and putting hold-downs in place. Sheathing thickness is based on how far apart the studs are, how much weight they need to hold, and what kind of material was used to build the wall. In fact, to the wall's component shear, the quality of the rafter material also affects the size and spacing of shear wall nails. The load is split between the bladders and the shear walls by the collectors, which are horizontal parts. Chords are vertical parts that hold the instant at edges of a shear walls. Figure 1-1 shows the typical shear wall assembly. It has framing bolts, sheathing boards, anchor bolts, hold-down devices, connectors between the sheathing and the panels, and end structural steel slabs.

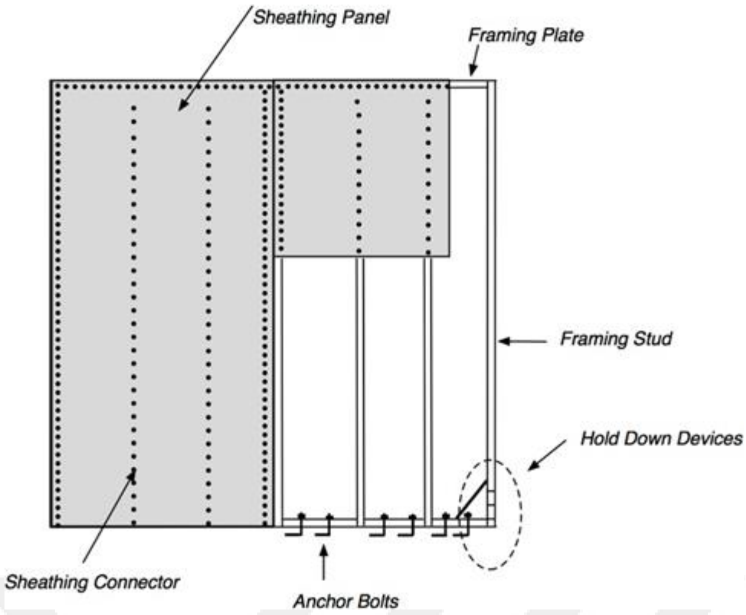

Figure 1.1 : Components and Connections For Shear Walls In The Frame.

1.3.2 Shear Walls with Lumber Structural Frames in a Wood Frame

Wood structural panels are extensively used in wood-frame shear walls (OSB or plywood). SDPWS and the International Building Code (IBC) list the unit developing a complete of shear walls made of wood structural panels. There are different capacities for wind, seismic, and some other different kinds of dynamic forces. IBC and SDPWS both agree that there are three possible ways to design shear walls for timber shear wall buildings. As the name suggests, segmented shear walls are cantilevered shear walls. They are used to think of the full-height wall elements between window and door openings as shear walls. Only the ceiling mount segments are expected to be able to handle lateral loads. Each of these parts must be built in a different way to account for the base moments and the compression or force applied inside the chord members that go with them. Each end of such wall fragment has a take connector.

The "design of shear forces around openings" method looks at the wall as a whole, including the holes for doors and windows. The second way to plan. Coupling beam: Timber shear wall segments behind and in front of an opening are thought to move vertical shear throughout the opening. As part of the special detailing, there will be more sheathing, nailing, and blocking. Like the other methods, the "perforated wood-frame shear wall method" uses the whole wall segment to figure out the design resistance. Capacity improvement factor Co.

is being used to account for how walls with holes lose strength and stiffness, but it doesn't say anything about how force moves around holes. If the second and third design methods are to be used, all parts of the shear walls that can be covered must be covered with structural panels.

1.3.3 Timber Framing Shear Walls Have The Following Chord Members

At the base, the force of turning is turned into angular compression and tension, which are both stopped by studs at the ends of a shear walls. So, these vertical studs, which are located at regular intervals, carry the longitudinal loads. Live loads, in addition to the axial forces that result from seismic overturning moments, can also contribute to the design loads that are placed on the chord members. By avoiding the extra importance load, one can reach a design for the tension chords that is more conservative. On the other hand, by removing dead loads, one can achieve a design for the compression chord members that has lower design loads. As a result of the vertical component of the earthquake shaking, chord members may be subjected to higher design loads than originally anticipated.

1.3.4 Design for The Anchorage of Wood-Frame Walls

To create a dynamic compressive force that can support both vertical gravity loads and shear forces that are lateral towards the walls of the building, there are a number of components that need to be connected to one another. The shafts and walls of the construction or something like it are held up by joist connections, which transfer the weight of the building trusses to the structure's components. In the same manner, the actual columns are connected to the column headings.

Shear wall plates made of wood are utilized to connect the studs; alternatively, the foundation may be utilized in order to attach the columns. To transfer shear to a substructure, anchor bolts are installed within the timber shear wall plate. Connections around the chords are utilized to convey gravity loads that are the result of a factor in deciding for lateral loads that are parallel to the walls.

1.3.5 Description of The Issue

Shear walls in constructions may have holes like doors or windows in order to achieve architectural aims. Due of the apertures' reduced lateral rigidity, the building's overall fundamental period has changed. Designers frequently overlook the impact of openings in walls when using finite element programs to create and analyze structures. In seismic design, ignoring these apertures could lead to erroneous results because of the illusory effects. It is also possible to create an unrealistic natural period for shear wall constructions by ignoring the opening effect when estimating the fundamental period of these structures using the coding formula.

1.4 AIMS OF THE INVESTIGATION

The following are the study's overarching goals:

a. Examining the effect of shear wall opening widths on the basic periods of shear walls structures.

b. Finding the smallest possible opening-to-sidewall ratios that can be overlooked when simplification is a goal in the design of the building.

c. Designing models that are as basic and safe as feasible by determining the lowest opening ratio required for the wall to behave like a frame.

d. Comparison of finite element and ASCE7-16 code results for approximating the basic period of shear wall structures.

e. Using statistical regression of the finite element findings to estimate the increase in the period of the shear-walled buildings owing to openings in the shear walls.

1.5 HYPOTHESES

The only foundation for this argument is comprised of the following hypotheses:

a. Because of the linear behaviour exhibited by the material, it is entirely possible to disregard the influence of yielding. This opens the door to the possibility of that.

b. P-delta effects are not going to be taken into consideration in this investigation in any way. When a structure or structural component experiences a significant lateral displacement because of lateral loads, it is conceivable for the structure or component to undergo rapid shifts in ground shear, overturning moment, and axial force distribution at the base of the structure.

c. According to the requirements of the ACI318M-14 code, the slabs and the walls must each have a thickness of twenty centimeters.

d. We are going to proceed with the assumption that the slabs are two-way flat plate slabs.

e. The assumption is made that the cross-section of each column is in the shape of a rectangle.

f. Because of the concrete that they employ, each individual member has a compressive strength that is equal to 24 MPa.

g. The calculations indicate that the superimposed dead load has a value of 4,000 newtons per square meter.

h. Absolutely nothing other than square shapes are permitted for the center window openings.

i. When viewed along its horizontal and vertical axes, the building can only appear to be in a square layout. When the center of mass and the center of stiffness are positioned in close proximity to one another or when the space between them is extremely minute, the typical case will be observed. This will be the case whenever either of these conditions is true.

j. The discourse that we are going to have is going to be structured around the primary mode that was determined by the modal analysis.

k. In the simulation, shell-thin elements are utilized so that they can accurately represent the slabs and shear walls.

1.6 METHODOLOGY

We will begin by going over the research that has already been published, and then we will learn about other methods that can be utilized to validate the results obtained using the finite element method. Additionally, we will acquire a deeper comprehension of the factors that influence our capacity to accurately estimate the basic period of shear wall constructions. As a computation instrument for this thesis, a third-party software package that is commercially available and is based on the discrete element method will be utilized.

The research will make use of two different degrees of simulation, which are as follows: At the "wall level," where parameters such as concrete compressive strength, wall geometry, and opening size all play a role, a detailed examination of the fundamental period of a single wall is performed. At the second level, also known as the "building level," the influences of opening ratio, building height, and stiffness ratio on the period and stiffness of three-dimensional buildings with regular distribution of planar shear walls are investigated. These buildings have a regular distribution of planar shear walls.

The ASCE7-16 code formula for determining the fundamental period of shear wall buildings will be applied, with the ratio serving as an estimate of the fundamental period of shear wall structures. In order to determine the impact that openings have on the basic period of shear wall constructions, it will be required to make a comparison between the modal periods of walls and buildings with openings and those that do not have openings.

Before being implemented in practical settings, programs for finite element analysis need to be subjected to stringent quality assurance inspections. This procedure will be followed throughout both stages of the research project. The manual estimation of the wall's flexural and shear deflections will be carried out as a component of the study, and the findings of this endeavor will be compared to those produced by the computer program. The computation for the deflection will take into account not only the solid walls but also the openings in the walls. It is allowed for there to be a discrepancy of up to 5 percent between the deflection findings generated by a human and those obtained by a computer for a wall that is solid. However, it is acceptable for there to be a difference of up to 25 percent for walls that include openings. In Rayleigh's method, the "building level" will need to be manually calculated before proceeding with the calculation of the period. It is not a cause for concern to have a difference of opinion of up to ten percent between the findings of manual analysis and the outcomes of program analysis.

1.7 THESIS LAYOUT

Chapter One: Is an overview of the study, which includes a description of the issue, the goals of the research, the scope of the work, and the methodology.

Chapter Two: presents the results of study done in the past.

Chapter Three: The author explores the methodology for modelling individual concrete walls with a variety of opening ratios. In addition to this, it studies the effect that the wall aspect ratio and the compressive strength of the concrete have on the lateral deflection of the wall. The purpose of this is to determine the ratio at which shear deformation can be ignored. The effect that the opening ratio has on the lateral deflection of the wall will also be covered in this section. This chapter illustrates when a solid wall will operate as a frame by analyzing models of various door opening widths. Specifically, the chapter focuses on door openings of varying widths.

Chapter Four: Provides results, Analysis, Discuss, give the final result that used by the methodology listed in Chapter three

Chapter Five: provides results, recommendations, and ideas for future research that will be used to expand on the current study that was conducted. As a consequence of this, these tests are essential in order to guarantee that the software generates precise results.

2. LITERATURE REVIEW

2.1 INTRODUCTION

In this chapter, reinforced concrete shear walls of varying types, connection connections, and failure mechanisms are investigated in order to achieve a deeper comprehension of how these structures behave when subjected to seismic loads. In addition to this, a review was conducted on the numerical analytical techniques for a parched precast part.

2.2 LOADBEARING SHEAR WALL BUILDING POST-SEISMIC PERFORMANCE

The most frequent and cost-effective method of resisting lateral force is the reinforced concrete shear wall. It is built to withstand lateral forces and keep the building from swaying from one floor to the next. High lateral strength, stiffness, and deformation capacity are all provided by the shear wall. Damages caused by inter-story drift are minimized thanks to the shear walls of the building. The construction of a shear wall, even if basic, is expensive, and there has been a push to make the wall system more cost-effective." Structures with shear walls that function well in earthquakes have been extensively documented (Fintel and Fintel 1995; Wallace and Moehle 1993; Wood et al. 1987; Wylie and Filson 1989). The use of precast technology, rather than traditional cast-in-place building, has resulted in cheaper construction costs, faster construction, and better seismic performance for concrete structures. The 1994 Northridge earthquake in California (Mitchell et al. 1995) and the 1995 Kobe and 1999 Kocaeli earthquakes in Turkey (Sezen et al. 2003), as well as the most recent 2012 Emilia earthquake in Italy (Yin et al. 2009), all had severe damage to precast building and bridge structures compared to monolithic reinforced concrete structures (Mitchell et al. 1995). (Magliulo et al. 2014). Joint connections were found to have a significant impact on the structural integrity and performance. Despite the fact that many precast structures were destroyed in Armenia during the Spitak 1988 earthquake, some precast constructions performed admirably despite the poor construction methods used (Wood et al. 1993). The lack of mechanical connectors between precast and monolithic elements resulted in the collapse of 60 percent of the precast industrial structures that were not designed with seismic requirements during the Emilia earthquake. As a result of the devastating 1995 earthquake in Kobe, certain precast and prestressed concrete structures performed well. Cracking was seen in cast-in-situ buildings, but precast walls behaved substantially better than cast-in-place walls, Figure 2.1.

Figure 2.1: Collapse of Precast Building.

During the Canterbury 2011 earthquake, a precast structure with an imitated design performed better than expected (Fleischman et al. 2014). It was possible to see firsthand the actual seismic performance of modern concrete structures during the Canterbury earthquake in 2011. The quake's devastating effects on Christchurch's structures and economy were documented in the city's official records. Pre- and post-1995 design standards were used to create the cast-in-place and precast concrete (emulated design) structures. Despite the fact that no RC structures fell in the Darfield earthquake, 40 percent of the 65 RC structures surveyed showed signs of damage, including fissures in major structural sections. ATC-20 Procedures for Post-Earthquake Safety Evaluation of Buildings Damage Assessment (ATC-20) Twenty-five percent were flagged as "red" and twenty-five percent as "yellow" (Fleischman et al. 2014). The Christchurch earthquake caused moderate to severe damage to post-1980s RC-buildings. The lateral system, floor diaphragm, staircases, and cladding were particularly damaged. NZ$30 billion was the total economic loss. Only the damage to precast and cast in place concrete buildings, which were not collapsible, cost the economy billions of dollars.

Because of the use of reinforcing steel and cast-in-place concrete (Kurama et al. 1999) and the fact that emulated joints sustain significant damages, forming plastic hinges within the precast member and dissipating large amounts of energy, the emulated precast structure design does not have the economic advantages of precast concrete construction. during the 1988 Armenia earthquake, the building with precast concrete walls as the major lateral force resisting system performed better than the building with another structural system. (Wylie and Filson 1989). Even while certain precast structures performed better than others after the earthquake, the vast number of damages detected in precast structures limited their application in seismic regions, Figure 2.2. As a result of precast concrete structures' poor performance, which was attributed to faulty design connections, there is now a lack of confidence in precast structure design and construction.

Figure 2.2: Damages to The Moment Frame That Has Been Precast.

2.3 PRECAST STRUCTURE CODIFICATION

Precast/Prestressed Concrete Institute (2010), Precast Concrete Buildings in Seismic Areas (fib 2016) and American Concrete Institute (ACI) ITG 5.1-07 are some of the codes used for precast concrete structure design. (ITG 2007). These standards recommend that precast structures be designed and reinforced in the same way as cast-in-place reinforced concrete structures, but with additional consideration for connections. For wall-to-wall connections under tension and shear, the PCI Design Handbook (2010) provides guidance on how they should be designed. The ACI 318-14(2014) joint connection design criteria include mild steel for yielding, with the yield strength of the non-yielding mechanical connector having nominal strength 1.5 times the yielding steel and intended for 80% of yield strength, as specified. The area immediately surrounding the joint connection necessitates a unique design due to the potential for significant stress and deformation. A discussion of precast systems' design philosophy and force transfer mechanism is presented by Fib (2016), explaining principles for the transfer of compressive, tensile, and shear forces with the use of bending. There are two ways to design joint construction in the NEHRP (FEMA 2015), all of which are acceptable. Both the emulation approach and the dry joint connection using mechanical connectors can be used to build joints that behave like cast-in-place concrete structures. Precast concrete applications in seismic regions are restricted by building standards in the United States Uniform Building Code (1997), the NEHRP Recommended Provisions, and the International Building Code (1997). A monolithic structure must have lateral load characteristics that are at least as good as those required by these regulations for analyses and testing. Cast-in-place emulation was created as a result of these codal providing needs (Ghosh 2002). As a result of the wet joint, precast loses its economic and speedy construction advantages. To prevent plastic hinges on the precast part, the joints are engineered to avoid inelastic deformation within the joints. This results in an unaffordable precast concrete member design. The majority of precast structure design codes focus on emulating joint design rather than limiting themselves to ductile design.

2.4 JOINTS IN PRECAST CONCRETE BUILDINGS.

The joint connection mechanism determines how well precast wall panels transfer lateral loads. Consequently, a precast structure's ability to withstand earthquakes is entirely dependent on the joint connection system (Magliulo et al. 2014; Tsoukantas and Tassios 1989; Vintzeleou and Tassios 1987; Brunesi et al. 2015). The failure of a precast construction can be attributed to weak joints, which weaken the structure's rigidity (Clough 1985; Seckin and Fu 1990). There are various ways to classify the joints between the precast connecting members.

2.4.1 Joints That are Both Wet and Dry

It can be classed as either a wet or dry joint depending on the usage of cast insitu concrete. Wet joints in precast structures use cast-in-place concrete, whereas dry connections use mechanical connectors including such bolts or welding to connect prefabricated members. The mechanical joints and damages on the edges of precast wall panels are the most vulnerable to damage from dry joints. There are two types of joints: those that are dry and those that are wet. When damaged, wet joints resemble a monolithic shear wall because of their increased stiffness and strength. When a dry joint is used, the stiffness and strength of the joint are significantly reduced, and the drift is much greater because of the plastic deformation solely in the joints. High seismic locations use wet joints, while regions with low and moderate seismicity use dry joints. Seismically active areas have begun using hybrid joints, which combine post-tensioning tendons with energy dissipation techniques. Although a wet junction increases rigidity and stiffness, it sacrifices the speed and cost savings that come with precast construction when compared to a dry connection method.

2.4.2 Durable and Sturdy Joinery

On the basis of its design philosophy, the precast structural system can be categorised as follows:

a. Strong linkage.

b. Connections with ductility.

Emulated design connections are another way to describe a strong link. Plastic hinges or inelastic deformation is created outside the joint position because of the rigidity and strength of the joints themselves, which are meant to be stronger than the precast part. Similar to typical monolithic construction, strong joint connection precast structures behave similarly. Modern precast moment-resisting frames still adhere to this design principle. In this way, the precast member is developed with strong joint connection features based on the current monolithic member design codes. When using a cheap connector, the plastic hinge is formed by the force of the ductile connection, which protects the pricey precast concrete member. The hinges are moved from the precast part to the less expensive joint connection system using this technique. Using a ductile connector, a precast concrete member can be connected to the building system to manage the inertia of the structure. Non-emulation design construction is another term for the ductile connection's design philosophy, which differs significantly from the emulation approach.

2.5 AN OVERVIEW OF THE PRECAST PROJECT WITH REGARDS TO SEISMIC STRUCTURAL SYSTEMS

In order to broaden the application of precast construction, the United States of America and Japan collaborated to launch the PREcast Seismic Structural System (PRESSS) program. Even though the technology of precast concrete has the potential to completely change the way buildings are constructed, it was not extensively used. The major objective of the effort was to produce comprehensive and practical design guidelines for precast structures in wider seismic zones. This would allow the initiative to achieve its core goal. Increasing the seismic range of precast construction can be accomplished through the development of new materials and technologies (Priestley 1991).

The study that is done on precast structures today can trace its origins back to the pioneering work of this team. Some of the motivations underlying the PRESS efforts that were initiated in the early 1990s are still valid today, thirty years after they were first conceived of.

a. The use of precast concrete blocks in construction is the method of the future. The use of components that are mass-produced and a construction procedure that is more rapid inspires new ideas in the design and construction of architectural and technical projects. In the not too distant future, more advanced robotic and AI technology will make it possible to better control quality and create structures using methods that are more efficient.

b. In spite of the evident potential it possesses, precast construction has a very limited capacity in terms of actual construction capacity. This technological advancement hasn't been put through its paces that much as of yet!

c. The ambiguity in the seismic performance of precast concrete engineering structures is the root cause of the low degree of comprehension that these structures have. Due to a lack of relevant expertise and appropriate experimental data in freshly completed construction, the use of precast construction was restricted in seismic regions.

d. The problem was made worse by design codes that called for experimental data as a kind of design validation. In order for precast constructions to satisfy the criteria of the codes, their performance needed to be at least as excellent as that of cast-in-place structures.

e. In light of the findings of this research, the development of a design method for precast seismic structural systems is an absolute necessity.

Experimentation and analysis were a part of the second phase of the PRESSS program, which focused on developing a ductile joining system for precast concrete parts. The strategy was suggested for use in a number of different earthquake zones. The PRESSS program's four different ductile connection types were ultimately chosen for implementation. These connections will allow for the precast frame and wall panel structures to be attached to one another. The many different kinds of connections are broken down into their most fundamental forms here.

a. Unbonded post tensioning is necessary for the creation of a ductile connection inside a non-linear elastic connection system. This can only be accomplished through the use of unbonded post tensioning. In this particular link, an elastic response that possesses non-linear features predominates. Even when the building is shaken by a significant tremor, this particular type of joint lessens the amount of damage, stops any residual drift, and gives the structure a high initial rigidity. The drift, on the other hand, is enhanced as a result of the effective damping being reduced. The level of equivalent viscous damping at ten percent is lower than that of structures made of reinforced concrete or steel.

b. Connectors that Have Yields Under Both Tension and Compression (TCY) In the event of an earthquake, connections made of medium-strength steel are designed to fail in both tension and compression in the direction that is diametrically opposed to the shaking. The behaviour of the hysteric curve is analogous to that of a monolithic reinforced concrete structure with a viscous damping of thirty-five percent. However, after the inelastic reaction, this system has a large residual displacement but a low residual stiffness. This is because the system has been deformed. A shear key or rough surface is provided to the contact surface of the precast member in this system. This is done so that excessive shear deformation at the interface can be avoided.

The combination of non-linear elastic and tension-compression yield connection systems has led to the development of a new type of connection system known as a hybrid connection system. An additional layer of damping is added to the primary connection by using post-tensioning made of mild steel as a tension-compression yield element. The linked system generates a hysteric response that is characterized by enhanced damping, residual stiffness, and little residual drift.

c. Bringing Together the Shear Yields In this particular system, moment rather than shear is responsible for activating the non-linear elastic connection system as well as the tension-compression yield connection system. These connections are illustrated by instances such as midspan beam connectors and vertical precast panel joints.

d. Coulomb Friction Connection Systems: These energy dissipation devices are used to dampen the system by connecting it to the connection. When coupled with a linear elastic connection, the connector's hysteric activity exhibits bilinear elastic-plastic behaviour.

Program Phase II included numerous experimental programs to test for the ductility of precast frame connections (Priestley 1996). Slender precast shear walls were examined by Schultz et al. (1998) as a lateral load resisting solution for precast buildings. Jointed precast structures have greater ductility and energy dissipation capability due to the inelastic deformation of the connections, It was the goal of the study to find a way to employ a portion of the concrete construction joint material to offer deformation capacity and energy absorption while minimizing damage to the concrete structure and anchorage. Precast shear wall connections were evaluated using numerous types of joints, such as grouted splice sleeve connections, post-tensioned tendon connections, precast vertical joints, and debonded smooth bars.

For precast concrete shear wall, Kurama et al. (1996, 1999) suggested the code definition for the post-tensioned tendon joint connection system. Precast concrete structures with post-tensioned connections in beam-column joints can be designed using an analytical method proposed by EI-Sheikh et al. (1999). When subjected to seismic loads, the unbonded post-tensioned precast frames resulted in greater maximum displacements than an equivalent monolithic reinforced concrete frame.

As part of a seismic design, Priestley and colleagues (2002) devised a method known as Direct Displacement Based Design (DDBD). Precast concrete buildings were able to be designed to withstand earthquakes at the design level with specified displacement limits, which corresponded to acceptable damage limit states. A 60 percent scale, five-story precast concrete building was designed using the DDBD technique and tested under seismic loads during the third phase of the PRESSS program. Post-tensioned tendon connection systems were used in the beam-column join and shear wall, and damping was given by mild steel reinforcing bars in select joints as a hybrid connection system. Based on the research of two earlier phases of the PRESSS program, the joint system was developed. A thorough description of the structure can be found in Nakaki et al. (1999) as well as Priestley et al (1999). In spite of a seismic intensity 50 percent higher than the design level, the precast building sustained only little damage. Only at the base of the walls was there some modest spalling of concrete. Framing damage was less severe than that sustained by a monolithic reinforced concrete structure that drifted in the same direction. Predictions of the building's response were made using mathematical models, which showed strong correlates to the test results. For the design of precast structures' joint systems, the PRESSS program provides an analytical method and a wealth of experimental data. The PRESSS's success drew researchers from throughout the world to study precast structural joint systems, and it also promoted the use of precast structures with ductile connections in seismically active countries.

2.6 DAMAGE PREVENTION APPROACH TO DESIGN AND STABILITY OF THE STRUCTURE

During the earthquake, the modern reinforced concrete structure built in accordance with the design requirements operated as predicted. In the Christchurch earthquake of 2011, no RC structures collapsed, which shows that this is the case (Fleischman et al. 2014). Repairing minor to severe damage to structures was expensive and took a long time, thus they couldn't be occupied for a while. It is imperative that modern structures are able to withstand small and easily repairable damage during earthquakes. Detailing the plastic hinge sections in this way will accomplish this goal. Limited strength and great displacement capacity are hallmarks of modern earthquake design. With significant displacements, the energy expended by the development of plastic hinges produces serious damage that is impossible to repair. "Damage Avoidance Design" was born as a result of this. The theory of "Damage Avoidance Design" was proposed by Mander and Cheng (1997) for the design of bridge piers. Reinforced concrete bridge piers utilize plastic hinges at the ends of bridge columns to dissipate energy. After a significant earthquake, the structure's hinge zones were severely damaged and required the substructure to be replaced. Because of the ductile design philosophy for large earthquakes, the damage was unavoidable. There are no longitudinal reinforcing bars at the beam-column interface in the DAD technique. There's a particular detail at the beam-column junction that lets the column rock.

Non-critical structural reparable elements are dissipated by the rocking motion of structures, preventing structural damage. It's a long-term method to designing structures in high-seismic areas. According to Housner, the concept for the rocking framework can be traced back to his work (1963). Aslam (1978) was the first to consider and Yim et al. were the first to quantitatively explore the use of prestress cable to anchor a rigid structure during ground motion (1980). The rocking mechanism of a rigid block over an elastic base subjected to ground motion was examined by a number of writers (Aslam 1978; Iyengar and Roy 1996; Lin and Yim 1996; Pompei et al. 1998; Yim et al. 1980). An airport chimney and a rail bridge in New Zealand are both examples of the genuine construction that has a rocking mechanism in it (Skinner et al. 1993). In 1993, Priestley and Tao conceived up the PRESSS program for precast concrete frame buildings with beam-to-column joint connections; in 1996, Priestley and MACRASE validated the program's findings. Beam-to-column prestressing cables experience a rocking mechanism at the interface when loaded from the side. Rocking motion caused the specimens to suffer less damage at large displacements than ductile connections. However, compared to a ductile connection, less energy was absorbed. Damage occurred due to significant joint cracking with concrete spalls at the beam's ends, but the ductile design performed better overall. Priestley and Tao, on the other hand, did not perform exactly bilinear as expected (1993). A modest modification in the structure's size, slenderness ratio, and ground motion characteristics had a significant impact on its rocking reaction (Lin and Yim 1996; Pompei et al. 1998; Yim et al. 1980). Post-tensioned tendons can be used to link precast parts such as bridge piers and beam-column connections (Alcocer et al. 2002; Billington and Yoon 2004; Dawood et al. 2011; Dawood and ElGawady 2013; Ou et al. 2007). Unbonded prestressed tendon systems were also connected to rocking shear wall systems (Erkmen and Schultz 2009; Henry et al. 2012; Holden et al. 2003; Hutchinson 1990; Pampanin et al. 2001; Perez et al. n.d.; Schultz and Magana 1996). Cracks appeared around the joint region and crushing and spalling of concrete occurred on the connected system"s outside borders in the unbonded post tensioned connected systems. The edges of the concrete should be reinforced and given specific detailing in order to alleviate the problem of concrete crushing at the edges. Henry et al. (2012) used end steel columns on the edges of the shear wall system to prevent concrete from crushing. In order to avoid concrete crushing, Erkmen and Schultz (2009) used spiral reinforcing on the margins of the shear wall near the contact interface.

2.7 SYSTEM FOR CONNECTING JOINTS BETWEEN PREFABRICATED CONCRETE STRUCTURES

There has been a lot of effort on inventing new ways to connect the joints of precast structures. Non-emulated and emulated designs are available for the joint system. To mimic monolithic concrete construction, emulation design employs precast components. Damage avoidance and displacement-based design methods have been the focus of recent work on precast concrete structures rather than traditional simulation-based methods. Here, we've outlined the many types of precast joints:

2.7.1 Connecting System for The Sleeve

Based on ACI 318-11, the mechanical coupler with full rebar strength development can be used. Belleri and Riva observed cyclic activity on a grouted corrugated steel sleeve connection (2012). Grooved corrugated sleeve connections on cantilever columns were tested for hysteric performance by Popa and colleagues in 2015. The performance of a grouted sleeve connection system under tensile load was examined by Alias et al. (2013). Connection system failure results from bar slipping out of connector or fracture occurring outside of connector. The anchorage length has a direct impact on the failure mode. If the anchorage length is too short, the bar will slip, but if it is long enough, it will fail outside of the connector. Precast concrete shear walls with grouted sleeve connections for the primary reinforcing steel bars were tested cyclically by Peng et al. (2016). To match the moment capacity of a monolithic structure, the shear wall joint system was engineered to have a similar moment capacity. The sleeve was used to attach the reinforcing bar, which was then filled with mortar. There was a comparable breaking pattern on the precast shear wall compared to the cast-in-place shear wall. Using the ultimate section force approach, it was determined that the precast shear wall's ultimate loading capacity could be computed. Precast shear wall had a greater cracking displacement than a mortar-sleeve joint-connected shear wall, but the yield displacement was the same. Precast shear walls had lesser ductility. In part, this was owing to the difficulties in securing bar in the sleeve.

2.7.2 A Lap-Spliced Connector That Has Been Grouted

In order to mimic monolithic guest stars construction as well as the grouted tube connection, this technology has been developed. To connect the foundation and main precast shear wall, a lap-splice is used in which one of the bars is lodged into a grout-filled hole with a metal bellow. The spliced bars were protruding from the foundation of the shear walls.

This shear wall is then covered with bedding mortar and brought into place using pre-drilled holes in the main shear wall. This completes the construction of this wall. Figures 2.3, 2.4, 2.5 shows the metal bellows and metal mesh being grouted.

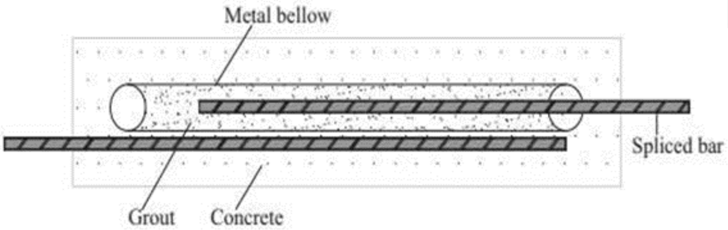

Figure 2.3: Grouting of Metal Bellow For Lap-Spicing.

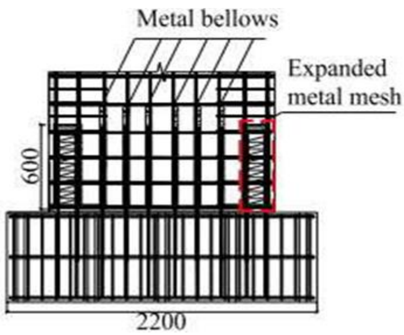

Figure 2.4: Lap Splicing For Reinforcement.

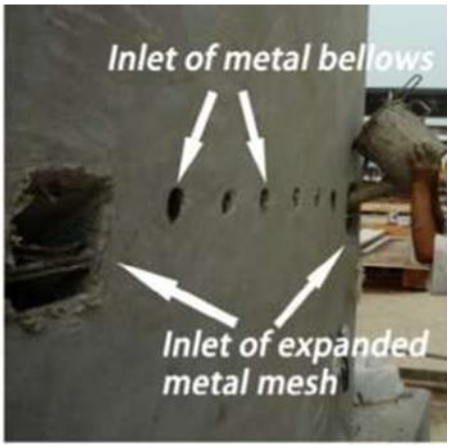

Figure 2.5: Process of Grouting.

2.7.3 The column dowel connection is made with dowels

Column integrity is critical for structural safety in precast frame construction. During the earthquake, faulty beam-to-column connections accounted for the bulk of precast frame construction collapses. Steel dowels have been the most frequent method of connecting beams and columns for decades. The dowel joint's strength, load-displacement behaviour, and failure modes have all been studied experimentally, Figure 1.6. Several authors have created numerical models to simulate the behaviour of dowels buried deep within concrete.

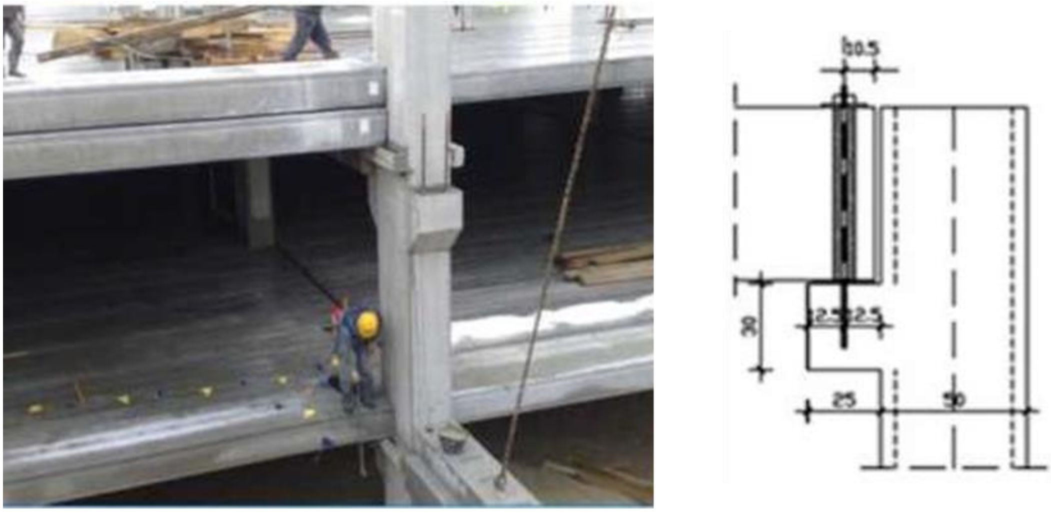

Figure 2.6:A dowel Connection Between a Beam and a Column.

2.7.4 O-connector

An O-shaped vertical connector made of mild steel instead of stainless steel was proposed by Sritharan et al. (2015) to maximize energy dissipation. The moment resistance of a multi-panel wall is lower than that of a single shear wall. A mild steel O-connector was offered as a replacement for the jointed wall system because of the drawbacks. More than one wall panel can be utilized with or without intervening columns if the aspect ratio is less than 2.0. The column's capacity to transfer gravity loads and simplify the design of the connector with a reduced maximum displacement requirement and lower fatigue make it a good choice. According to Twigden and Henry (2019), the energy dissipation by O-connector dissipater was studied using a shake table test. The O-connector dissipating measure with self-centering shear wall and end columns was studied by Henry et al. (2010), Figure 2.7.

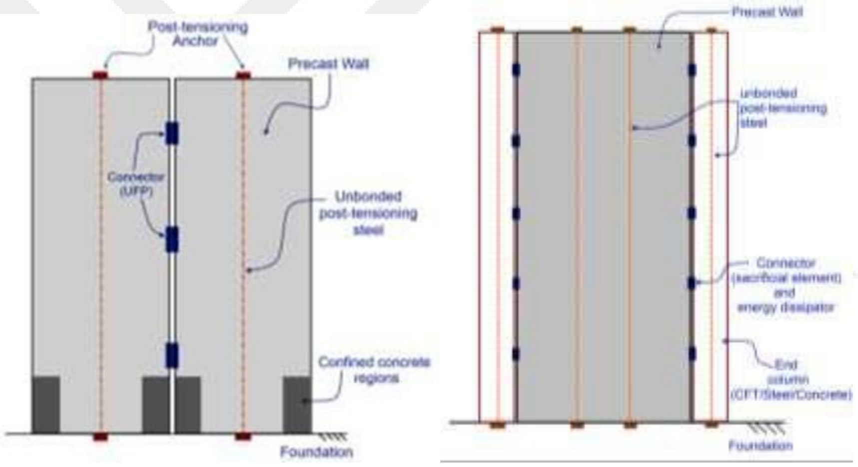

Figure 2.7: End Columns in a Precast Wall.

2.7.5 Fastened to H-Steel Section by Bolts

In Figure 2.8 shows the results of an investigation by Sun et al. (2016) on the mechanical joint connection in precast shear walls. H-steel was used to make connections between the shear wall and foundation more convenient. Shear wall was bolted with high-strength bolts over the whole length of the structure. H-beam connector buckling caused the breakdown, which in turn led to crushing of the concrete around the margins.

Figure 2.8: Shear Wall with Bolts and an H-beam Precast Concrete.

2.8 THE CASE OF A DAMP GROUT JUNCTION

Dry joint connection behaviour in precast concrete wall-based systems was extensively studied in the late 1980s. It was found that Rizkalla et al. (1989) studied forty-three specimens with fifteen distinct dry connection configurations to understand the various limit states of the horizontal connections under shear, cyclic shear, and cyclic shear/flexural stresses. Shear connections for load-bearing wall panels were examined by Foerster et al. (1989). A high-rise precast panel prototype had been created. The five types of horizontal connections were prepared:

a. Grout should only be applied with a dry pact.

b. Continuity bars and dry pact grout.

c. Type A shear connector and type A dry pact grout.

d. Shear connector type B and type B dry pact grout.

e. Use dry pack grout to shear the key.

One-to-one loading was applied to each specimen. Dry grout joints deformed significantly before cracking, whereas joints with continuity bars did not. Before shattering, the shear connector had no major impact on the joint's behaviour. When compared to a joint without a shear connector, the rigidity was gradually reduced thanks to the shear connector. Comparing a joint with simply dry grout to a joint with shear key increases the load carrying capacity. The degeneration of the joint surface caused the loss of rigidity. In comparison, the mechanical connector increased ductility by 80 percent, whereas the shear connector increased ductility by only 65 percent. PcaC wall panels were tested for shear resistance using multiple shear keys by Serrette et al. (1989) and a horizontal connection for precast wall panels was tested by Soudki et al. (1996) using a reversed cyclic shear deformation in conjunction with gravity loads. The integrity of the panel connections is critical to the operation of the precast concrete load-bearing shear wall panel structure during an earthquake. Only dry pack grout was used to make the connection. Also included were dry joint experiments using shear key, reinforcing bar welded to steel angle, post-tensioned strand, and post-tensioned bar. Crushing and spalling of dry pack grout caused all of the connections to fail under cyclic pressure, resulting in a reduction in grout thickness. Shear resistance was lost as the grout thickness was reduced. The hysteresis loops stabilized at reduced shear strength when the dry grout was crushed. The shear key dramatically enhanced the shear resistance while minimizing slip. This higher shear resistance can be attributed to the mild steel reinforcement's completeness. The connection's shear resistance was improved thanks to the prestressed reinforcement, which enhanced the connection's effective stress. A dry connection's shear resistance can be enhanced by supplying a key, raising the connecting member's tensile strength, or by increasing the effective stress normal to the connection. To generate shear keys using the dry pack connection technology, Figure 2.9 to 2.12 shows the particular preparation needed.

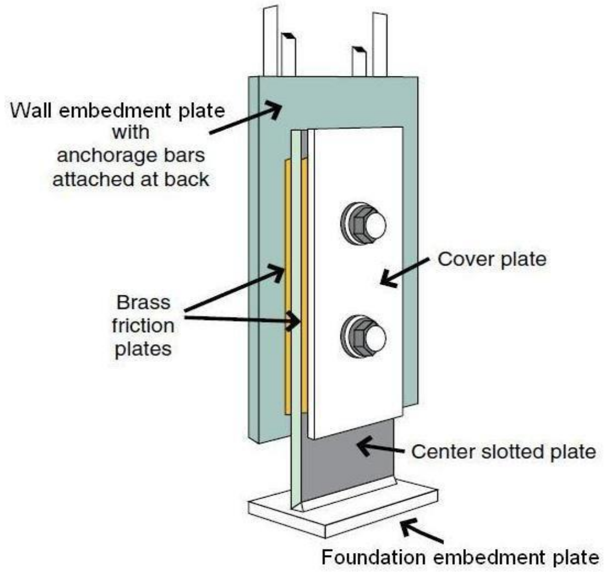

Figure 2.9: Connection Dry-Pack Grout Only.

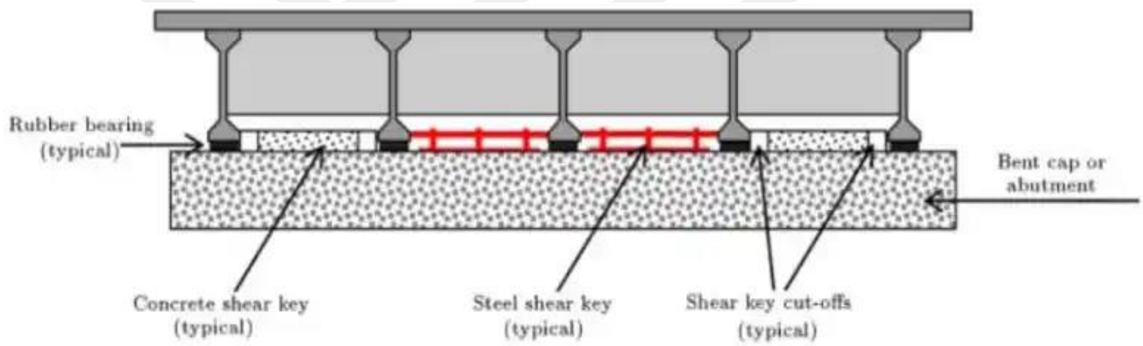

Figure 2.10: Connection Shear Key.

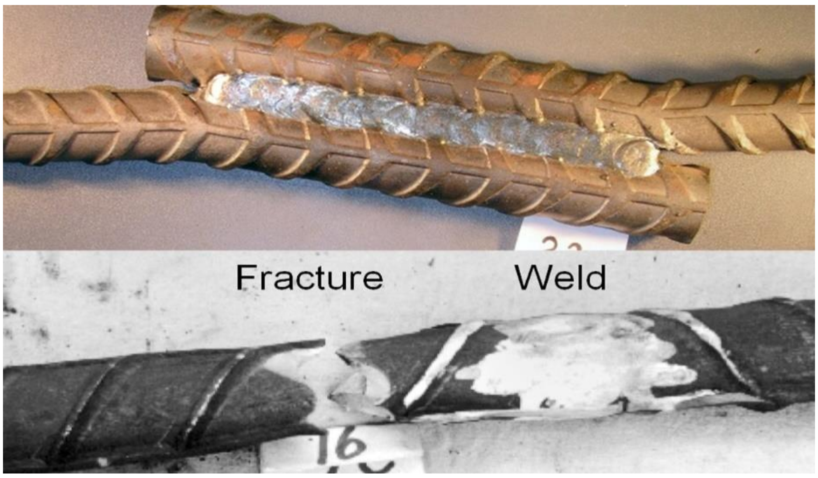

Figure 2.11: Welded Connection for Reinforcement Bars.

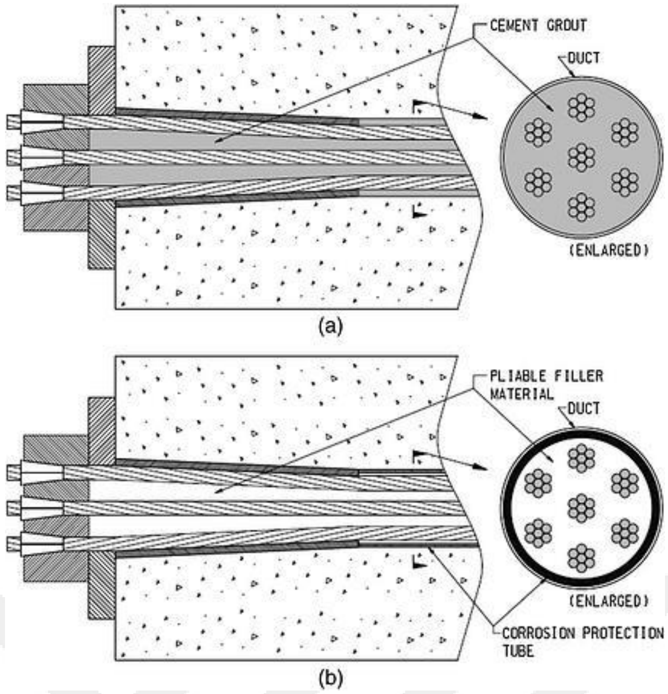

Figure 2.12: Utilizing Strands or A Bar to Post-Tension.

2.9 ANCHORED-BOLTED SYSTEM

To attach the shear wall concrete panels together, high-strength fasteners that are anchored in place are an option. The reliability of the joint connection system was evaluated using a shake table test on a three-story precast concrete wall panel building, and the results are depicted in Figure 2.13.

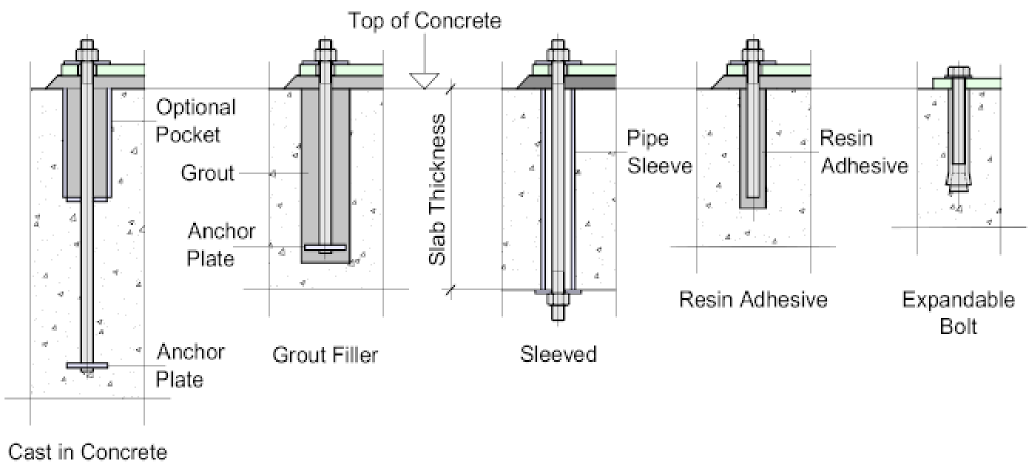

Figure 2.13: The Floor and The Wall Are Connected with A High-Strength Bolt That Is Fastened in Both Locations.

2.9.1 Bolt System

Chen et al. (2019) studied a bolt-assembled precast concrete panel building's seismic performance. Two-story building cyclic loading test. Zhong et al. (2019) studied a bolted beam-column coupling (Figure 2.14).

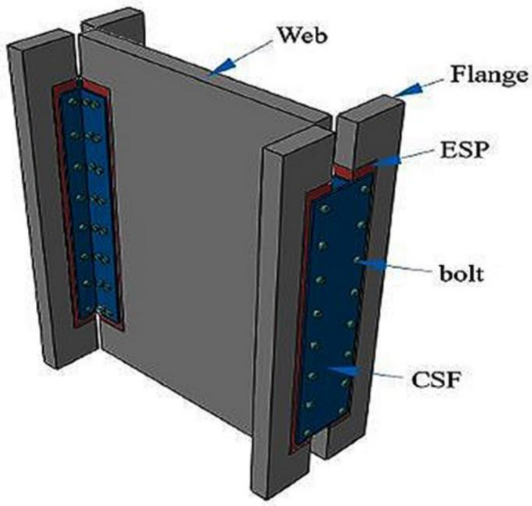

Figure 2.14: Ordinary Bolt-Connected Shear Wall System.

2.9.2 Connectors with Slotted Bolts

For a precast shear wall, Bora et al. (2007) advocated the use of slotted bolts to connect the member to the structure. Shear wall prefabrication is supported by a system of slotted bolt connections. The joint system's bottom is secured into the foundation or a wall to prevent it from moving about. The cyclic load causes the connecting system to slip and lose energy via friction. The anchorage failure is avoided by the elastic-plastic reaction of the slotted bolt connection, Figure 2.15.

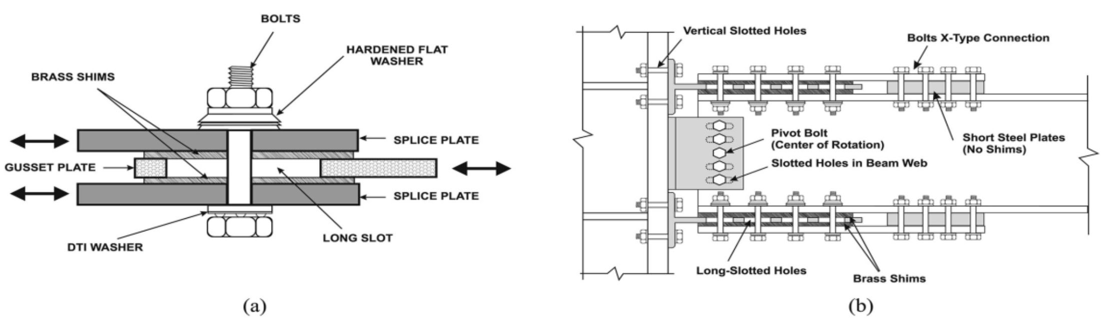

Figure 2.15: Slotted Bolt Connection.

2.9.3 A Mechanism of Tendon Attachment That is Post-Tensioned

The PRESSS program helped popularize the post-tensioned tendon joint attachment technology (Priestley and Tao 1993). These tendons are used to link the precast shear wall or beam column to each other. Limits are placed on any remaining horizontal movement by an elastic recovery force. The quantity of cracking in this system is smaller than in a monolithic member that is only bonded with reinforcement. The system's response is bilinear elastic. However, compared to monolithic systems, the precast part connected solely by unbonded post-tensioned tendons wastes a little amount of energy (Holden et al. 2003). Thus, a hybrid system using mild steel bars as a monolithic construction was developed to disperse additional energy.

2.9.4 Hybrid Means of Interfacing

As compared to an emulative joint connection, a fully post-tensioned tendon joint connection system in precast shear wall has a lower dissipation of energy. Thus, a novel joint system called as a hybrid joint was created by combining the advantages of post-tensioned tendon joint connection and emulative joint connection. A monolithic structure of mild steel bars is used as well as the connection with post tensioned tendons in hybrid precast shear walls. As an energy dissipator, mild steel bars inhibit the opening and closing of gaps in the post-tensioned tendon connection system during cyclic pressure. These low-carbon steel bars bend easily under tension and compression, allowing the stored energy to be dissipated (Smith et al. 2013). While the gravity loads operating on the wall give self-centering capabilities, mild steel bars are engineered to yield and disperse energy in order to maintain a stable structure. The hybrid system, which combines energy dissipation measures with a self-centering shear wall, has been the subject of numerous studies (Christopoulos et al. 2002; Gu et al. 2019; Ho et al. 2016; Holden et al. 2003; Hu et al. 2012; Kurama and Shen 2004; Sideris 2015; Smith et al. 2013). The self-centering shear wall has a greater drift capability than the standard monolithic shear wall. Shear walls with energy dissipating devices can lower drift demand while also increasing energy dissipation capacity. The self-centering hybrid shear walls proposed by Kurama (2002) are in addition to the design technique for self-centering shear walls (Kurama et al. 1999) and can be used at various levels of seismic energy. Kurama (2000) extended the design method to the self-centering shear wall with a viscous damper, and more study was done on energy dissipation measures for self-centered shear walls (Twigden et al. 2017; Twigden and Henry 2019). Figure 2.16.

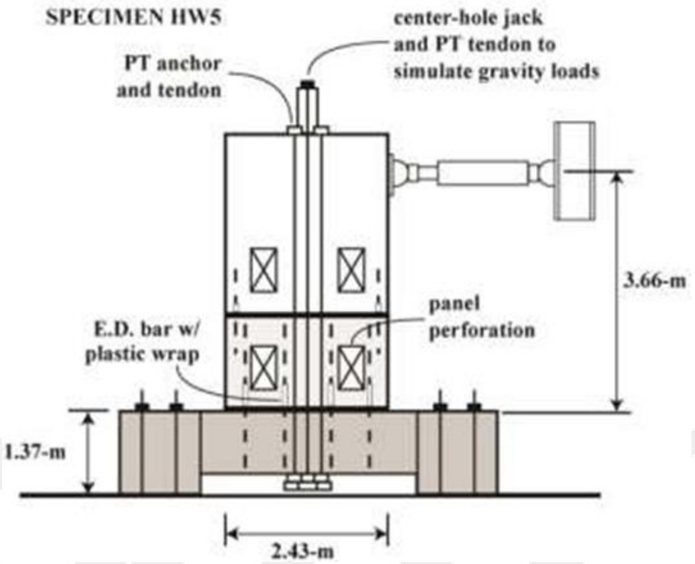

Figure 2.16: Post-tensioned Connection with Mild Steel Bars in A Hybrid Connection System.

2.9.5 Precast Wall with Joint Connection Numerical Analysis

In order to model the usual horizontal joint behaviour of a precast concrete shear wall with a rocking mechanism, Becker and colleagues (1980) devised a modelling methodology. Non-linear behaviour in the joint system was assumed to be limited to the wall panel, which remained in elastic phase. The joint's non-linear behaviour is caused by the connection opening, which causes the neutral axis to shift and the connection plane to slip. There is no slip between the contacting layers when the precast shear wall is rocked. The structure of the joint softens as the intensity of excitation rises. Sliding from one panel to the next was extremely rare. Around the corners of the wall panels, there was a noticeable concentration of force. Unless specifically engineered, the corners and connector ends of wall panels are subjected to substantial degradation. Due to the concentration of inelastic material just in the joint, the ductility of a wall panel is reduced as a result of the construction of a plastic hinge. As a result, it was suggested that the shear force in horizontal connections be kept substantially below the design's maximum capacity.

The analytical model developed by EI-Sheikh et al. (1999) was used to investigate the seismic behaviour of unbonded precast concrete frames. The beam-column interaction can be modelled using two alternative analytical models: the fibre model and the spring model. DRAIN-2DX (Prakash et al. 1993) was used to create these models. The fiber model consists of a variety of components: For example, elastic beam-column elements, truss elements, and zero length spring elements are used to model the linear elastic deformation of beams and columns, respectively, while a rigid link and rigid end zones are used to model the axial deformation and flexural deformation of the parts of the beams and columns within panel zones, respectively. Structural elements in fibre models are replaced with zero-length rotational spring elements in the spring model. They used EI-Sheikh et al. (1999) unbonded post-tensioned numerical model to test the analytical model formula and to compare with the current experimental results, which Perez et al. (2007) proposed as an analytic model formula and adopted.

The load-displacement relationship for a precast concrete frame with ductile connections was mathematically calculated by Pampanin et al. (2001). A five-story precast building created as part of the PRESSS program was used to test the process. Post-tensioned precast reinforced concrete frame buildings with rocking beam-column were modelled by Spieth et al. (2004). All that is needed to mimic the precast member's contact area is a compression spring attached to the pot-tensioned cable or bars. During compression, the neutral axis is at infinity, and the contact area is sealed. To begin opening a joint from infinity, the section's neutral axis moves along the plane of connection. Contact regions that are composed of extremely stiff materials will cause the member to rotate around their edges and not compress. The proposed rotational behaviour is seen here (Housner 1963). Concrete, on the other hand, isn't very rigid, which causes a compression zone.

Precast shear wall with prestressed connecting system was modelled by Palermo et al. (2005). A multi-spring element characterizes the beam-to-column or wall-to-foundation interaction. There is an accurate representation of how the neutral axis changes with time. Depending on the section's action, the spring's property is selected. Parallel elastic springs are used to describe curvature at the contact caused by cracking, as proposed by Palermo et al. (2005). A great deal of work has gone into numerically analyzing precast column rocking mechanisms (Khanmohammadi and Heydari 2015; Marriott et al. 2009; Palermo et al. 2005; Sideris 2015; Spieth et al. 2004; Wang et al. 2011). A numerical model on a self-centering frame was created by Lu et al. (2015) and seismic analysis was carried out.

To better understand the shaking of a column under monotonic loading, a FE model was created by (Abdelkarim and ElGawady 2014; Dawood et al. 2011; Dawood and ElGawady 2013; ElGawady and Dawood 2012). An FE study on the rocking behaviour of shear walls with post-tensioned tendons under cyclic stress was conducted by Khanmohammadi and Heydari (2015). Rocking mechanisms on shear walls or columns under cyclic loads may only be modelled using finite element analysis (FEA). Joint connection modelling is computationally expensive and difficult to get realistic pinching behaviour under cyclic loads due to its high non-convergence. For quasi-static monotonic loading analysis, 3D finite element analysis works well. Analysis by Sun et al. (2016) considered the contact between the foundation and the shear wall for monotonic loading. As a shell element, the H-beam was not subjected to contact simulation with bolts. In addition, the stiffness of the numerical model is quite high up to the yield load and is decreased by taking quick slip into consideration. The experiment, on the other hand, shows no sign of a sudden shift. In order to resist a horizontal load, Sun et al. (2019) did a FE study on two shear walls joined vertically.

2.9.6 Sandwich Wall Panels Using Precast Concrete Shear Wall.

In a dry joint connection, the shear wall remains in an elastic state. At 3% drift, there were a few obvious fissures in the experiment's results. As a result, the shear wall can be reinforced with the least amount of heat possible. The precast concrete sandwich wall panel can also be used with this. Thermal insulation can be achieved by sandwiching the insulating material between the concrete layers. An significant development in green energy construction is the sandwich panel. Composite, non-composite, or partially-composite concrete wall panels are available. The cost of heating and cooling the building can be reduced thanks to the insulation layered between the external and interior concrete layers. The moment of inertia of the section can be increased without increasing the thickness of the concrete shear wall by inserting insulating material between the concrete. For precast concrete sandwich walls, researchers Naito et al. (2011) investigated the performance and characterization of shear ties. Shear ties are used to join the various layers of external concrete. Precast concrete shear wall with the steel shear connector was researched by Benayoune (2007, 2008) for its axial load and flexural behaviour under axial loads and flexural strains. Glass fiber reinforced polymer shear connectors on insulated concrete panels were examined by Tomlinson and

Fam (2014) and Woltman et al. (2013). The increased thickness of the insulating layers resulted in a decrease in sandwich panel strength. It was Choi et al. who first used the corrugated GFRP shear connectors (2015). As part of their investigation of the concrete wythe's composite action, Salmon et al. (1997) tested a fiber reinforced plastic connector (FRP connector). Thin composite shear walls with high thermal insulation were studied by Voellinger et al. (2014). Concrete was layered between the vacuum insulated panels.

3. METHODOLOGY

3.1 INTRODUCTION

This study aims to investigate and investigate the effect of the shape and size of the holes made in the shear walls on the shear strength behaviour of single beams made of reinforced concrete specimens (which includes the deflection, cracking loads, and the maximum carrying capacity of the beam samples). Taking into consideration the effect of the compressive strength of concrete and the ratio of longitudinal reinforcement, this study aims to investigate and investigate the effect of the shape and size of the holes made in the shear walls. This study was done by simulation RC specimen (W15), which included the experimental work that was done on the specimen that we chose, and then designing this specimen by the finite elements using computer program, and then designing (6) similar models containing openings which they are different in number and shape then analysed them using the finite elements by ABAQUS software version 2019 , also make simulation between the results that we got from the computer program and the original model as a reference with the new models that have different opening .

3.2 EXPERIMENTAL PROGRAM

3.2.1 Specimen (The Validation)

Based on the previous research specimen, the W15, 2021 shear wall specimen was created as a simulation tool for use in design and analysis. The shear wall specimen stood a thousand millimeters tall and had a wall thickness of 150 millimeters. The shear wall shear strength ratio, the shear wall design ALR, and the shear wall HRR were the three most important variables in this experiment. The axial load ratio (ALR) is computed by dividing the axial force (which is positive for compressed and negative for tension) by the product of the axial compressive strength of concrete and the shear wall's total cross-sectional area. Several shear walls, for example, were built with HRB400 steel bars and C35 concrete. Hidden columns of the same length as the wall thickness are created by edge members made of 4C10 longitudinal bars and C8@90 stirrups inserted at both ends of the section. To apply axial load, a jack was placed on top of a loading beam created at the very top of the shear walls. The loading beam section size of the specimen loaded in axial compression was

300mm300mm, whereas the specimen loaded in axial tension was 500mm300mm. A foundation girder of 500 mm x 600 mm x 2000 mm must be built beneath the fastened shear wall specimen at its end. The top of the beam was lowered by 150 mm to accommodate the horizontal load. The specimen's precise specifications are shown in Table 1, and its dimensions, cross-section, and reinforcing structure are shown in Figures 1-3.

In addition to the wall specimen, three 150 mm 150 mm 150 mm concrete cubes were cast and subjected to the compression test to evaluate the compressive strength of the concrete.

Table 3.1: Parameters of Specimen.

Specimen	Height H (mm)	Width W (mm)	Thickness h (mm)	Horizontal Reinforcement		Vertical Reinforcement		
				SSR	HRR(%)	ALR		
W15	750	1000	150	C8@90	C10@90	0.75	0.75	0.3

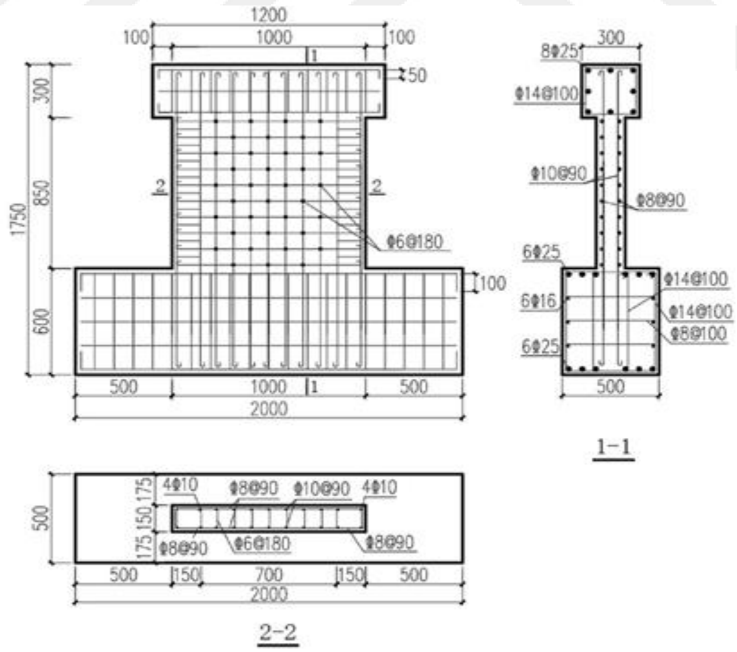

Figure 3.1: Specimen Geometry and Reinforcing Plans.

The axial compressive strength of concrete was put to the test, and the results showed an average value of 32.42 MPa. In Table 3.2, the results of a conventional tensile test, the yield strength and ultimate strength of three steel bar samples with the same diameter as the test specimen are displayed. This test was conducted using a conventional method. The objective of the test was to determine whether sample had greater yields and overall strengths than the other samples.

Table 3.2: Strength and Stiffness of Reinforcement.

Specimen	Diameter (mm)	Yield strength fy (MPa)	Ultimate strength fu (MPa)	Elasticity modulus Es (MPa)
W15	C8	429	556	2.0 × 105
	C10	453	570	2.0 × 105
	C12	499	605	2.0 × 105

3.2.2 Test Equipment and Method

The experimental loading rig consisted of a counterforce frame, two electro-hydraulic servo actuators from MTS weighing 150 tons each for the horizontal force, a jack weighing 500 tons for the vertical force, a ground anchor mechanism, auxiliary control hardware, and data gathering equipment. While the MTS electro-hydraulic servo actuators were responsible for the horizontal force, the jack was responsible for the vertical force. The loading apparatus that was utilized in the axial compression test may be seen in Figures 2 and 4, respectively. The ground anchor bolts of the foundation beam were utilized in order to anchor the base of the specimen, and additional support was provided by the counterforce piers that were installed on either side of the beam. The loading beam was attached to the end face of the MTS actuating cylinder by a screw connection, and a cushioned beam was used to connect the loading beam and the actuating cylinder. Because moving the loading beam to a new location was necessary, this action was taken. To guarantee that the axial compression force generated by the jack was being distributed evenly throughout the secondary wall and the hidden columns, a rigid cushion beam was positioned on top of the specimen. This was done by placing the beam on top of the specimen. A horizontal sliding support was installed in the space that was occupied by the vertical jack and the beam of the counterforce frame. By acting in this manner, we guaranteed that the vertical load would continue to be supported at the correct angle.

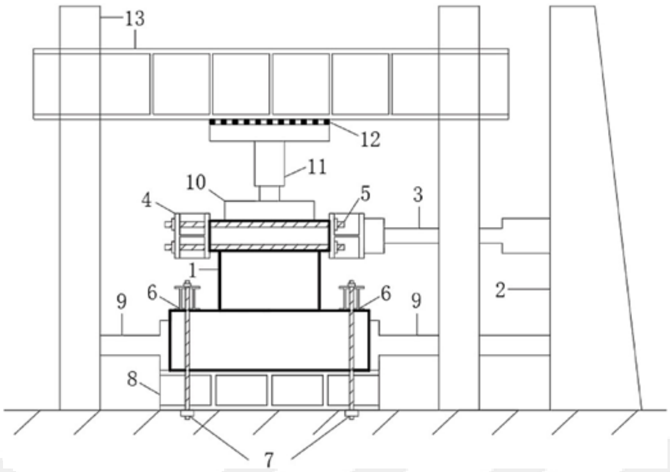

Figure 3.2: Apparatus for Loading Specimens that are Compressed Axially.

Apparatus for loading specimens that are compressed axially:

a. Specimen

b. Counterforce wall

c. MTS actuating cylinder

d. Cushion beam

e. Force transmission screw

f. Pressure beam

g. Fixed screw

h. Rigid cushion beam

i. Horizontal fixed beam

j. Rigid cushion beam

k. Hydraulic jack

l. Roller

m. Counterforce frame.

The testing technique began with the application of a steady vertical load. The specimen then underwent two phases of horizontal cyclic loading. The horizontal force was limited before the specimen fractured, in this case by increments of 100 kN. As the projected cracking load was neared, the force increments dropped. Following the cracking of the specimen, the horizontal displacement was limited to H/1000increments, where H is the height of the shear wall. Two cycles of loading were applied at each displacement level after breaking, compared to a single cycle before cracking.

3.3 OBSERVATIONS AND FAILURE MODE BASED ON

Shear sliding (SS) mode failure occurred in the shear wall specimen when it was subjected to both axial and horizontal shear stresses at the same time. The failure mechanisms and load and displacement values at the shear wall specimens' maximum and ultimate points are shown in Table 3 based on the average results from two loading directions. These numbers are the result of measurements taken in two separate loading directions on shear wall specimens. The load has reached its maximum, denoted by the symbol "Pmax," when it has taken up all of the available space in the system. When this happens, we say that the load is at its peak. Final point is defined as the time when the load is 85% of its maximum value. Pu represents the maximum allowable load of 0.85Pmax.

Table 3.3: Failure Mode Specimen.

Specimen	SSR	ALR	HRR	Maximum Load Pmax	Maximum Displacement Δmax	Ultimate Load Pu	Ultimate Displacement Δu	Failure
			(%)	(kN)	(mm)	(kN)	(mm)	mode
W15	0.75	0.3	0.75	617.96	2.06	525.27	3.17	SS

Figure 3.3: Observed Failure of Specimens with SS Failure.

Although having a very low maximum load bearing capacity, specimen W15 with SS failure possesses excellent energy dissipation capacity and substantially full hysteretic loops. This is due to the vertical steel bars at the sliding plane's dowel effect, which significantly contributed to the energy being dissipated as the specimen created a sliding plane at the base earlier.

3.4 EXPERIMENTAL TEST RESULTS

The specimen's horizontal load-shear displacement hysteretic curves are visible in the Figs below. Before applying the full force, the specimen experiences very little shear deformation. When the load is at its maximum, the shear deformation quickly rises along with the increase in displacement.

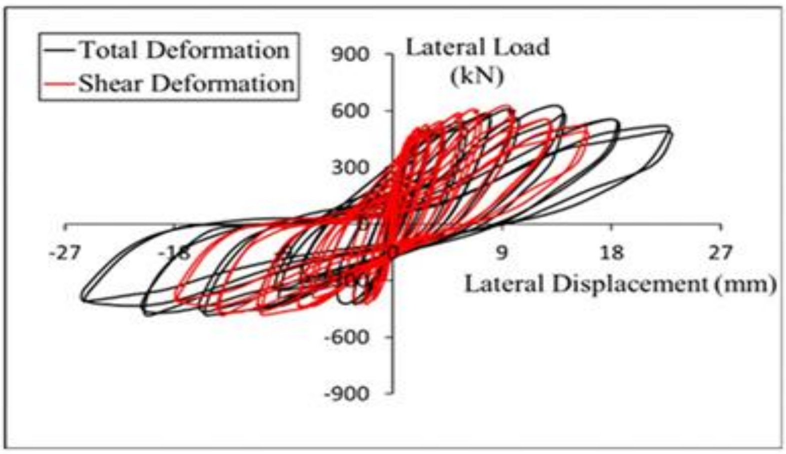

Figure 3.4: Specimens' Hysteretic Curves when The SS Fails.

3.5 MODEL OF FINITE ELEMENTS

We used ABAQUS 2019, a finite element tool, to study the response of reinforced concrete beams to changes in design parameters. The ABAQUS software can simulate any geometry and represent the linear and nonlinear behaviour of the vast majority of engineering materials thanks to its extensive library of element types and material attributes.

Concrete is a material assemblage often employed in engineering-related building. Experimental studies on concrete under uniaxial compression have revealed highly nonlinear tendencies, and modelling reinforced concrete has demonstrated similar results.

The next sections elaborate on the ABAQUS-based reinforced concrete beam modelling that has been presented thus far.

3.6 MODELING OF MATERIALS

3.6.1 Modelling of Constitutive Materials

Both the concrete damaged plasticity (CDP) and concrete smeared cracking (CSC) constitutive models are included in ABAQUS. The CDP model is preferred over the CSC approach because of the greater predictability it offers. In order to more precisely define the mechanical behaviour of RC beams subjected to a range of loading scenarios, it is common practice to utilize the CDP model that is supplied in ABAQUS. The damage plasticity model was used in this investigation.

Compression crushing and tension cracking are the two main ways that concrete, a brittle material, can fail. To acquire these processes and comprehend how they function, one can use the "Concrete Damage Plasticity" option in the ABAQUS software and choose the concrete material's compression and tension behaviour. Due to the fact that the failure and strength processes for compression and tension in concrete are different, two different uniaxial stress-strain relations were used for each. The relationship between stress and strain in concrete under uniaxial compression and tension was expressed using a number of different equations.

3.6.2 Steel's Typical Stress-Strain Behaviour

A typical stress-strain behavior of steel (hot-rolled carbon steel) is shown in Figure .

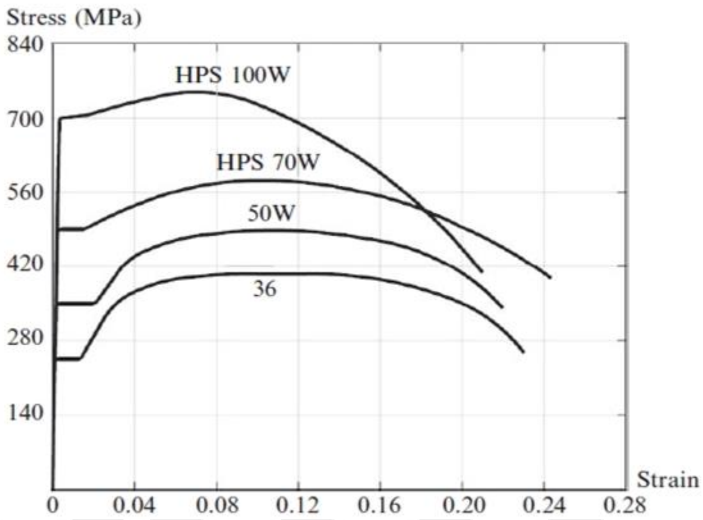

Figure 3.5: Typical Example Engineering stress – Strain Curves for American Bridge Structural Steels.

Proposed bilinear plus nonlinear hardening model together with typical experimental stress-strain curve. Stress Curve - Typical stress hot-rolled carbon steel has been subjected to Figure 1 shows the semi-static tensile load The slope is linear and is determined by the modulus of elasticity or Young's modulus E, 210,000 N/mm2 for structural steel was taken according to EN-1993-1-1 [13]. The linear path is limited by the yield stress fy f The corresponding yield strain is εy, followed by the plastic region.

It flows in almost constant pressure until the strain hardens εsh stress reached. At this point, the plastics production plateau ends Hardening strain begins. After this point, stress builds up Resumes at a reduced rate up to the maximum tensile stress fu and the corresponding final tensile strain εu, as shown in Figure 1.

$$f(\varepsilon)=\begin{cases} E\varepsilon & \text{for } \varepsilon \le \varepsilon_y \\ f_y & \text{for } \varepsilon_y < \varepsilon \le \varepsilon_{sh} \\ f_y+(f_u-f_y)\left\{0.4\left(\dfrac{\varepsilon-\varepsilon_{sh}}{\varepsilon_u-\varepsilon_{sh}}\right)+2\left(\dfrac{\varepsilon-\varepsilon_{sh}}{\varepsilon_u-\varepsilon_{sh}}\right)\Big/\left[1+400\left(\dfrac{\varepsilon-\varepsilon_{sh}}{\varepsilon_u-\varepsilon_{sh}}\right)^5\right]^{1/5}\right\} & \text{for } \varepsilon_{sh} < \varepsilon \le \varepsilon_u \end{cases}$$

3-1)

$$\varepsilon_u = 0.6\left(1-\frac{f_y}{f_u}\right), \quad \text{but } \varepsilon_u \ge 0.06 \text{ for hot-rolled steels}$$

(3-2)

$$\varepsilon_{sh} = 0.1\frac{f_y}{f_u} - 0.055, \quad \text{but } 0.015 \le \varepsilon_{sh} \le 0.03$$

(3-3)

As for the curve of typical cold formed steel stress – strain , it differs with hot formed steel stress – strain curve in a slight way and there is no stage in it of Perfect Plastic , and in most cases the elastic modulus is somewhat weaker and the ultimate stress is also relatively less, and the difference between them by fy is less than in hot rolled steel .

3.6.3 Steel Reinforcement Characteristics

As can be seen in the figure, this study made use of the ABAQUS software to do a simulation of the steel reinforcement using an elastic perfectly plastic material. It is sufficient to say that perfect plasticity denotes that the stress at the material's yield point does not change as a direct result of the plastic strain. Table 3.4 outlines, for your perusal and reference, the mechanical characteristics of the steel reinforcement, both longitudinal and transverse reinforcement included. Both the Poisson ratio and the modulus of elasticity are assumed to be 0.3 and 2,000,000,000 MPa, respectively.

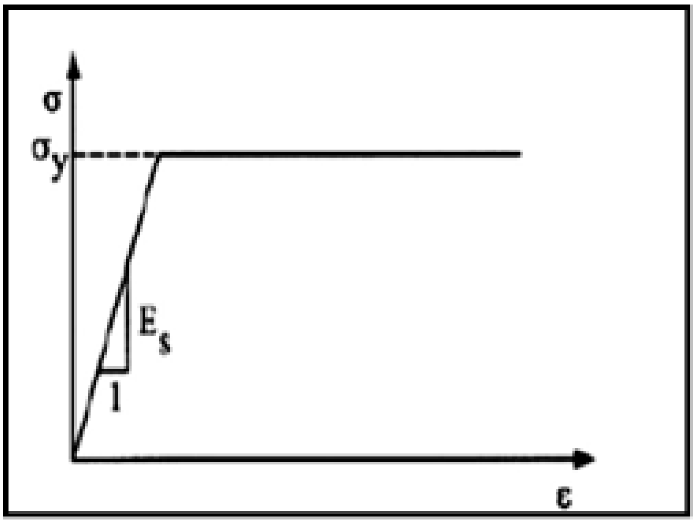

Figure 3.6: Steel Reinforcing bar Elastic Properly Plastic Model.

Table 3.4: Steel Reinforcement is a Variable Input.

Nominal Diameter (mm)	6	8	10	12	16
Yield Stress (MPa)	420	420	420	420	420

3.6.4 Concrete Uniaxial Displacement Stress-Strain Idealization

Figure 3.7 depicts a common example of the stress-strain behaviour of concrete when it is subjected to uniaxial compression.

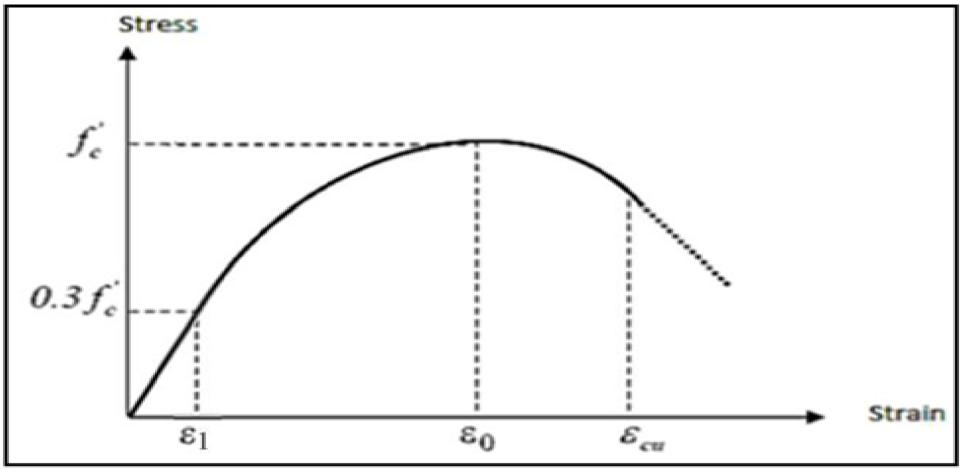

Figure 3.7: Concrete's Uniaxial Compressive Stress-Strain Curve.

At approximately 30% of the ultimate concrete compression strength (fc), the trajectory becomes nonlinear. The stress curve in the linear portion demonstrates a progressive increase in curvature until approximately (0.75 fc to 0.9 fc), after which it bends more abruptly as it approaches the maximum value. The stress-strain curve flattens until the point of failure, which is caused by concrete compression at the ultimate strain (cu) (Leet and Bernal, 1997). In accordance with the criteria of the ACI 318M-19 code for the compressive ultimate stress, the strain at the select stress, which was determined to be 0.002, and the ultimate strain, which was determined to be 0.003, were determined to be 0.002 and 0.003, respectively.

The following equations were required to determine the stress-strain curve for multilinear isotropic concrete. These equations were derived from a compressive stress-strain relationship for the concrete model.

$\varepsilon 1$ = Strain at (0.3 f_c),

ε o = Strain at peck point.

ε cu = Ultimate compressive strain.

3.6.5 Concrete Uniaxial Tension Stress-Strain Idealization

An indirect tensile test was performed in accordance with (ASTM C496-04) to establish the tensile stress corresponding to failure under tensile loading. After a linear stress-strain relationship has been attained for a distance of about 0.6 feet in concrete subjected to uniaxial tensile stress, micro-cracking propagation and the subsequent formation of a continuous crack system at peak stress cause the stress-strain curve to diverge from linearity. The development of a continuous fracture system is responsible for this nonlinearity. The material then enters the post-peak region after the occurrence of an unstable micro-crack system that develops rapidly under tensile stress. The strengths here are noticeably lower than those at the summit. For concrete under uniaxial tensile stress, the stress-strain relationship is shown in figure (3.8).

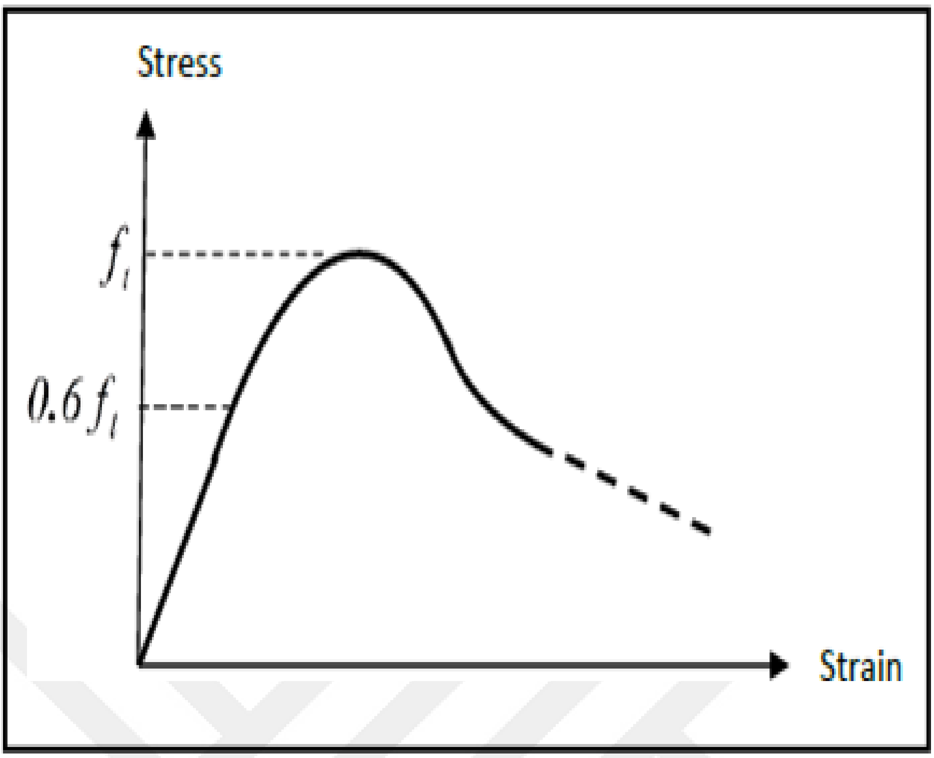

Figure 3.8: Concrete's Uniaxial Tensile Stress-Strain Curve.

In addition, this curve was generated by modifying the formula that was produced by (Wang and Hsu, 2001), which was then used by Kmiecik and Kamiski to construct the curve. The curve continues to rise linearly until it reaches the Cracking Failure Point (CFP). The curve eventually begins to descend in a steady manner and assumes the shape of a parabola. The following is a breakdown of what this behaviour looks like:

a. $f_{cr} = 0.31\sqrt{f`c}$

b. $\varepsilon cr = fcr/\ Ec$

c. $ft = Ec.\ \varepsilon t for\ \varepsilon t < \varepsilon c$

d. $ft = fcr\ (\varepsilon cr/\varepsilon t)^{0.8}$ $\quad for\ \varepsilon t > \varepsilon c$

3.7 INPUT DATA

There are five elements of the CDP framework that need to be defined, including the following:

a. The eccentricity of the hyperbolic flow potential (ε), which denotes the point where the hyperbolic flow potential approaches its asymptote. In ABAQUS, the default value is 0.1.

b. Viscosity parameter, the relaxation time of the vicious system. The default value given in ABAQUS is zero, but to improve the convergence in some problems, a small value can be.

c. The ratio of the tensile meridian's second stress invariant to the compressive meridian's second stress invariant such that the maximal principal stress is (-kc), another description (is one of the parameters for determining the concrete plasticity model yield surface) The initial value of kc in ABAQUS is 0.667. The results indicate that kc might be anywhere between 0.5 to 1.

d. To calculate the FBO/FCO ratio, we divide the initial equiaxial compression yield stress by the starting uniaxial compressed yield stress. The ABAQUS factory setting is 1.16.

e. The dilation angle (ψ) is the slant of the plastic potential versus the applied stress. The valid range of in ABAQUS is 0^o to 56^o. Concrete becomes increasingly brittle as the dilation angle decreases. For this study, an enlargement angle of 31^o degrees was chosen.

In Table 3.5 is where the defined values for the ABAQUS damage plasticity simulation for concrete are presented for reference. Notably, the control specimen examinations for each concrete's strength that were performed during the experimental work defined the values that were used for each model's concrete attributes.

Table 3.5: Specifics on The Concrete Utilized in the ABAQUS simulation.

Component	Description	Value
Elastic	ɣc, kg/m3	2451
		2492
	Ec, MPa	31625
		37741
	υc	0.2
	fˊc, MPa	45
		65
Plastic	Eccentricity	0.1
	Viscosity parameter	0
	kc	0.667
	fbo/fco	1.16
	Dilation angle, degree	31

3.8 MODELING IN GEOMETRIC

All the finite element models of this inquiry were assembled into four components, as follows:

a. Figure (3.9) illustrates the relationship between beam length and concrete section dimensions.

b. The process of reinforcing the tensile steel beam, as depicted in Figure (3.9) of Chapter 3.

c. Figure (3.9) from Chapter 3 depicts the reinforcing of the stirrups at the beam ends.

d. The plate of steel that will serve as the load bearer and support structure in Section 3, as depicted in Figure (3.9).

Drawing the cross sections of the beams was the initial stage in the process of producing the pieces. A three-dimensional solid component depicted the beam made of concrete, while a three-dimensional wire component portrayed the reinforcement made of steel. The graphics that accompany this text provide visual representations of each individual component that was modelled with a finite element.

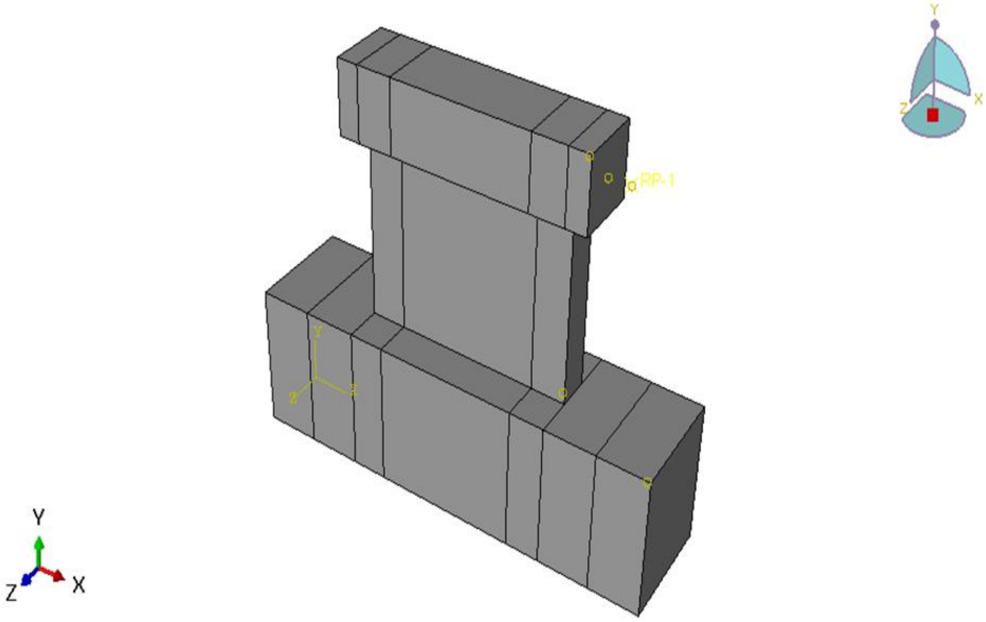

Figure 3.9: Modelling Beams with ABAQUS Software.

3.9 TYPES OF ELEMENTS

essentially, the analysis's accuracy, execution time, and precision of outputs are all impacted by the element type chosen for the FE analysis. A linear brick with eight nodes, a reduced integration element, and an hourglass control (abbreviated as C3D8R) were used to model the structural components of the concrete in this study. This element, which may define plastic deformations, cracking, and crushing of concrete, has six degrees of freedom (translation in the x, y, and z directions) at each node, as shown in Figure (3.10). The shorter overall execution time was a major factor in selecting the smaller integration component. This element was also used to model the steel plates that carried and supported loads in the model.

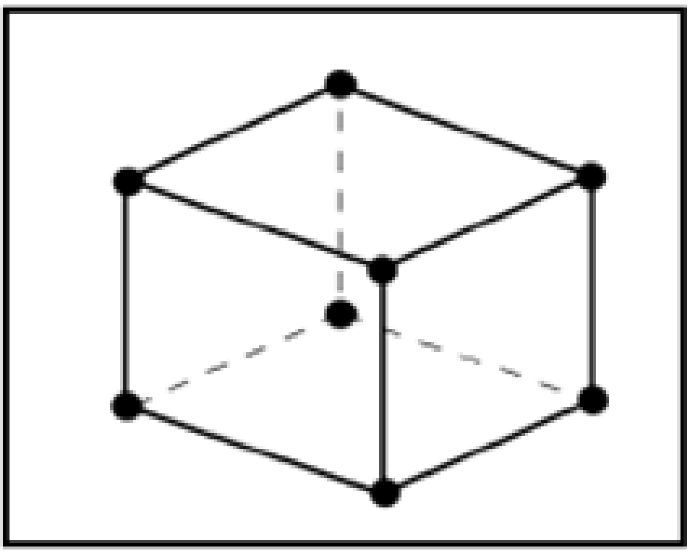

Figure 3.10: Element C3D8 is a Solid with Eight Nodes.

The truss element T3D2, also known as a 2-node linear 3-D truss element, is depicted in the figure. This particular element was selected to symbolize the steel reinforcement, which consists of tensile steel and web bars. In ABAQUS, this element can be used to provide the structural element that is responsible for the transfer of axial forces exclusively.

For the purpose of simulating the rebar-to-concrete bond-slip behaviour, embedded units have been developed within the main unit. After the embedded units have been defined, ABAQUS will search the nodes of the embedded units and the main units for any geometric relationships that may exist between the two sets of units.

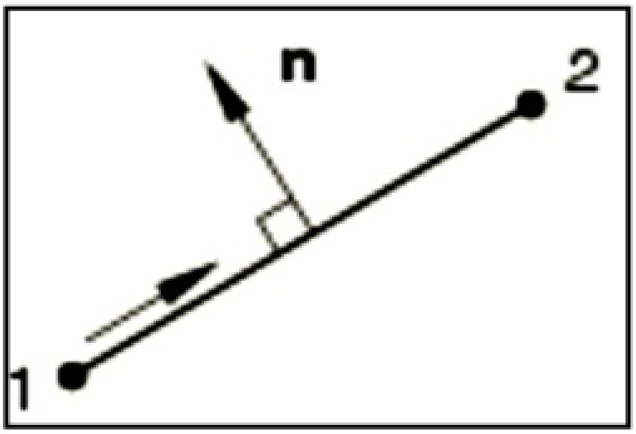

Figure 3.11: T3D2 is a Truss Element.

3.9.1 Modeling with a Mesh

After completing the Assembly module, mesh sizes for the models of reinforced concrete beams were chosen based on the efficiency and accuracy of the computations when compared to the results of experiments. The principal steel bars and stirrups employed a mesh size of 20 millimetres, while the concrete utilised cube elements measuring 15 millimetres. As can be seen in Table 3.6, the range of concrete and steel reinforcing element counts that resulted from the different cross sections of the reinforced concrete beam specimen models was determined by the beams' cross sections.

Table 3.6: Adopted ABAQUS Model's Total Number of Elements.

Type	No. of elements
C3D8R Linear hexahedral elements	13439
T3D2 Linear elements	1023

3.9.2 Surface Interactions

It is widely acknowledged that one of among the most important variables that affects the accuracy of outcomes is the modelling of the interaction between the various components. Using the “embedded region” option included in the ABAQUS software, the researchers in this study modelled the reinforcement made of steel and the stirrups to have a perfect connection with the surrounding concrete. This was done so that the results of the study could be accurately interpreted. On the other hand, the "tie" constraint is used to represent the interaction between the concrete and the loading plates, whilst the "Penalty" friction formula was used to simulate the interaction between the concrete and the supports, and the friction coefficient was set at 0.74. During the analysis, these members will continue to be totally connected to one another and will act constantly if you use this constraint.

4. RESULT AND DISCUSSION

4.1 INTRODUCTION

Within the realm of structural engineering, the use of numerical approaches is pervasive to find approximation resolutions to challenges that are particularly complex. The strategy that is being discussed here is referred to as the Finite Element method (FE method). In most cases, it reduces the size of individual structural parts to an extremely minute level. Analysis using nonlinear finite elements frequently produces accurate estimations of the findings of structural output and can accurately account for the fundamentals of structural analysis and design theory. Recently, FE analysis has become increasingly popular, particularly because of the advancements that have been made in computer technology. This chapter covers the process of developing three-dimensional nonlinear finite element models of reinforced concrete (RC) beams that are subjected to shear behaviour. The ABAQUS program, version 2019, was used to construct and analyze these FE models. According to Hussein et al. (2016), this program, which was developed for use in general engineering, is capable of finding solutions to a wide variety of linear and nonlinear problems. The concrete-damaged plasticity model was utilized to do the calculations necessary to determine the nonlinear material behaviour of concrete. From the experimental testing beams result for the concrete compressive strength (f′c), splitting tensile strength (ft), and Elasticity Modulus (Ec), appropriate input material parameters were supplied.

All the structural aspects of reinforced concrete beams, including their material characteristics, boundary conditions, loading techniques, and surface interactions, were discussed in extensive depth. To evaluate the outcomes of the experiments, the load-deflection relationships as well as the cracking patterns of the reinforced concrete beam models were recorded and compared to the findings of the experiments.

4.2 MODELS WITH FINITE ELEMENTS

The researcher designed, using the computer program, a similar model for the purpose of simulation, and then made openings with different shapes and dimensions for the purpose of comparing them with the original model and with each other through the curves of the load displacement. the table below illustrate the models opening shape and their dimension.

Table 4.1: Numerical Models Opening Shapes and Dimensions.

No	Opening shape	Opening dimension (mm)
1	circlular	150
2	rectangular	201*350
3	square	266*266
4	2 circular	106
5	2 rectangular	266*133
6	2 square	201*201 175*175

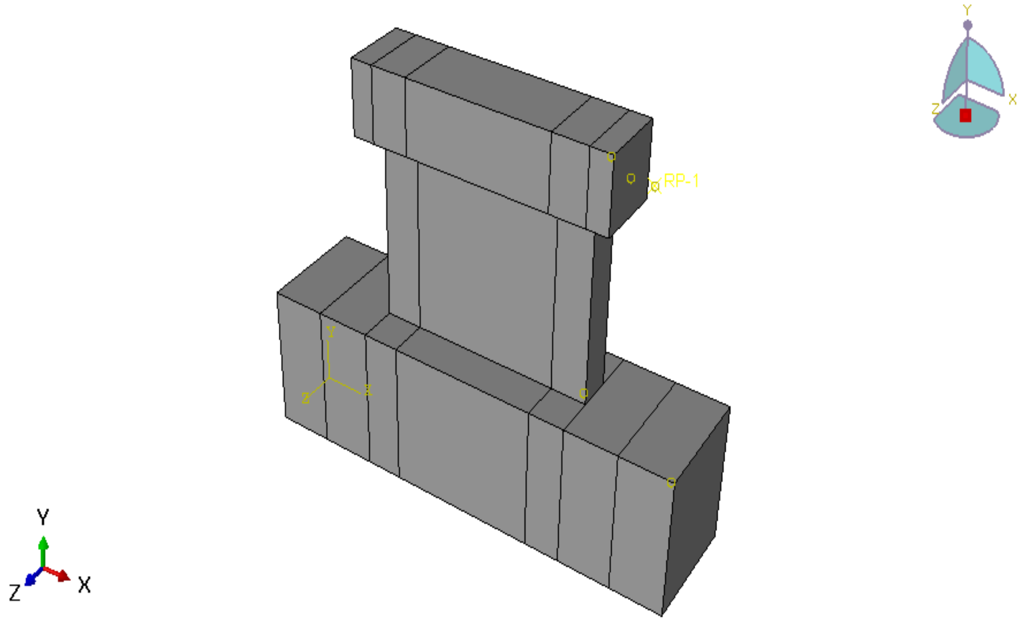

Figure 4.1: Shear Wall Solid Model in ABAQUS Software.

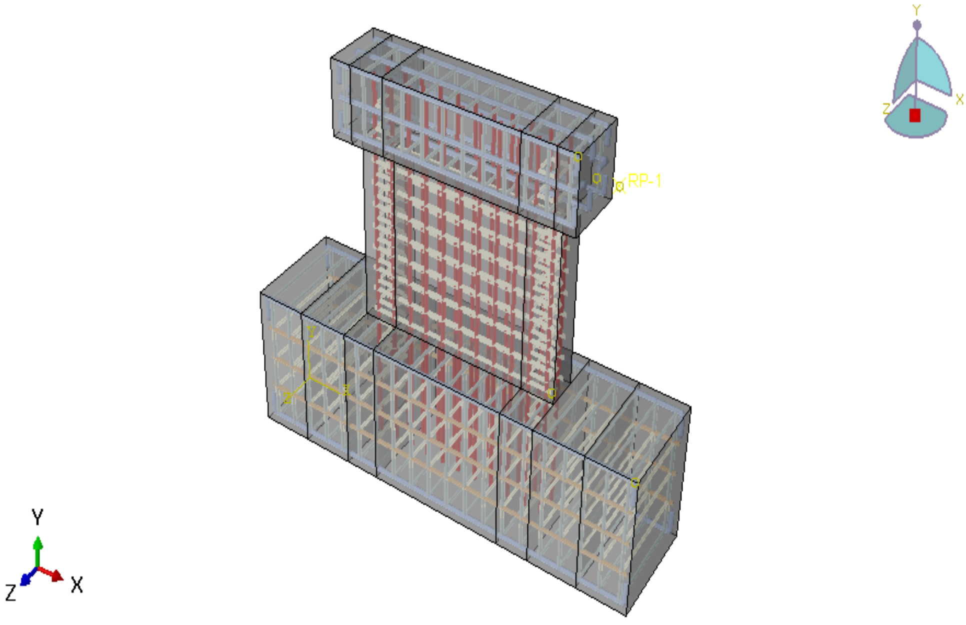

Figure 4.2: RC shear wall Model in ABAQUS Software (a).

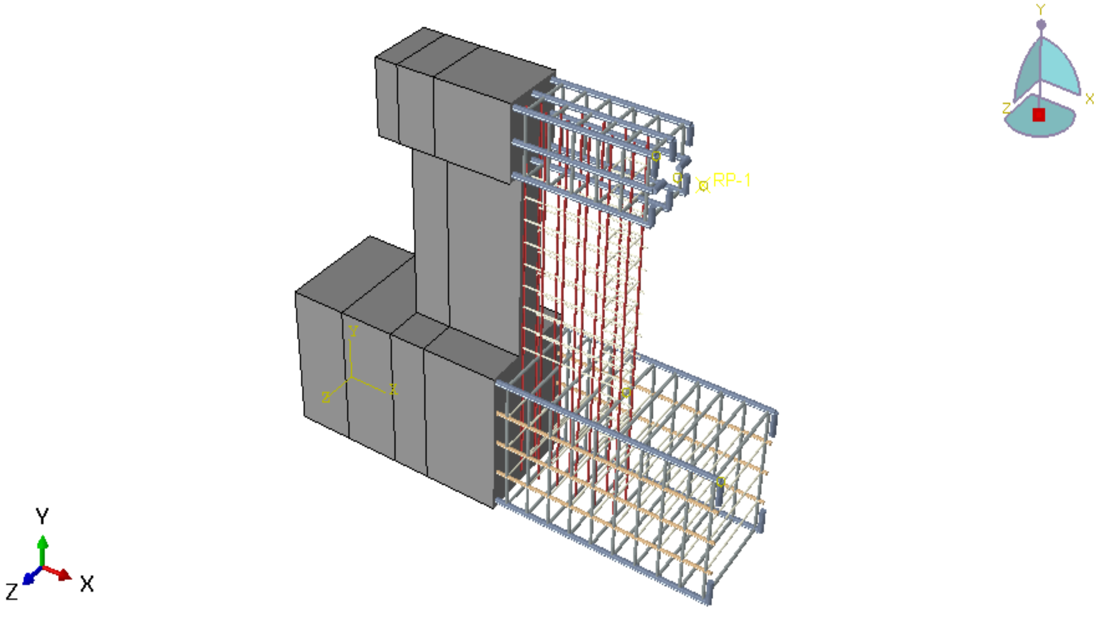

Figure 4.3: RC Shear Wall Model in ABAQUS Software (b).

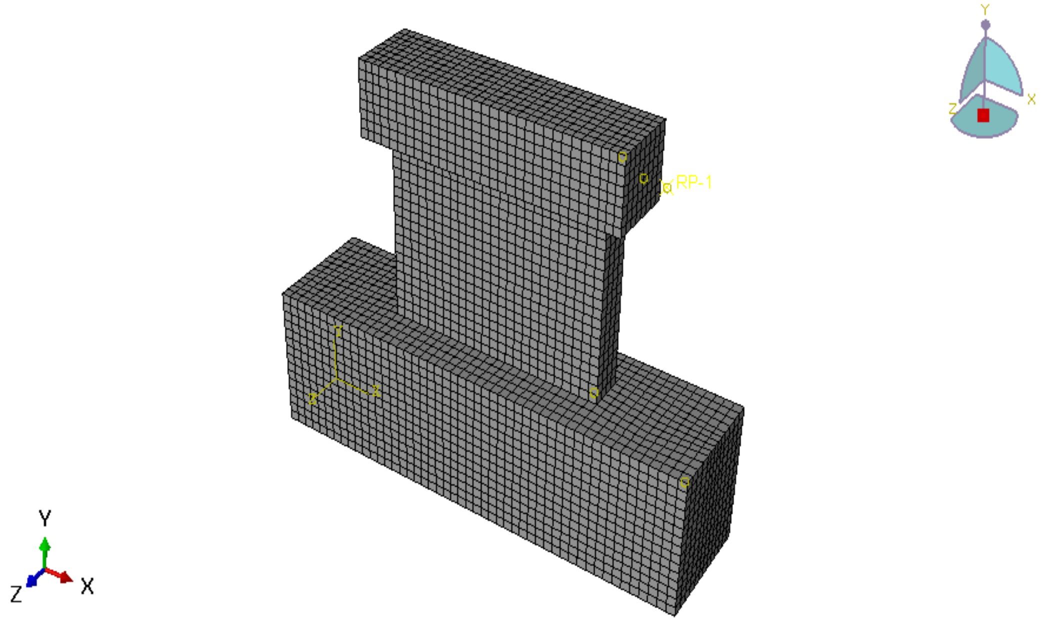

Figure 4.4: RC Shear Wall Model in ABAQUS Software in Mesh Status.

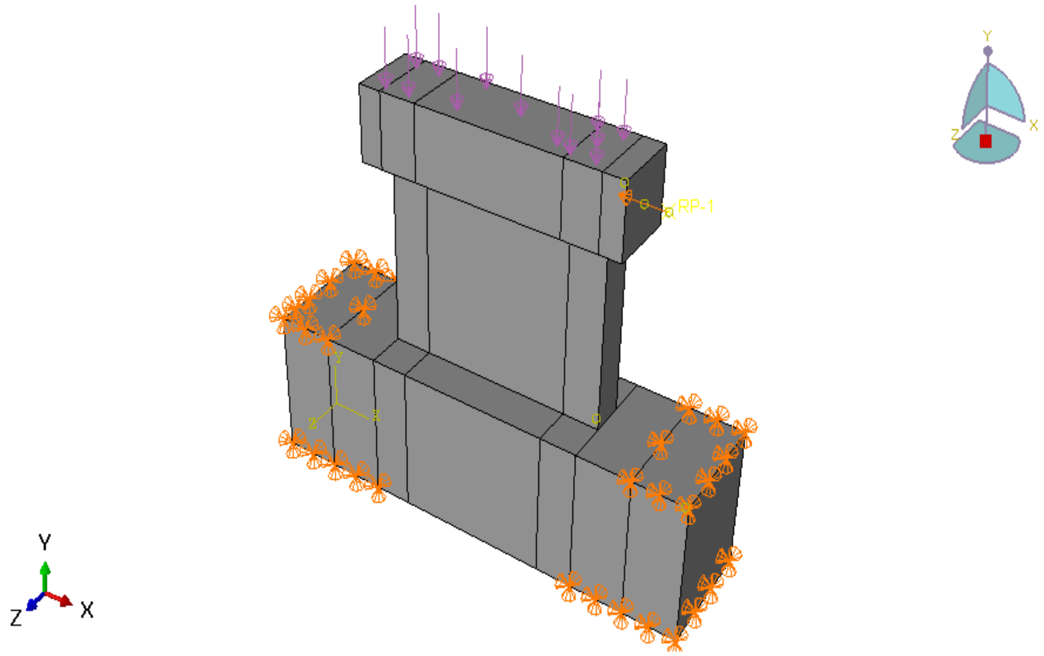

Figure 4.5: RC Shear Wall Model Under the Effect of Loading in ABAQUS Software.

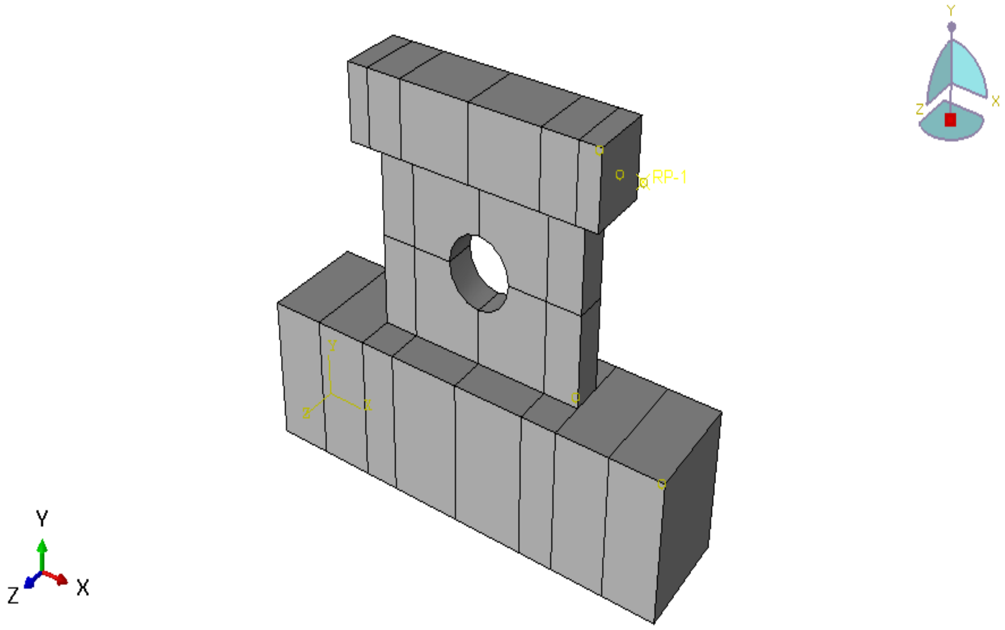

Figure 4.6: RC Shear Wall Model in ABAQUS Software with One Circular Opening.

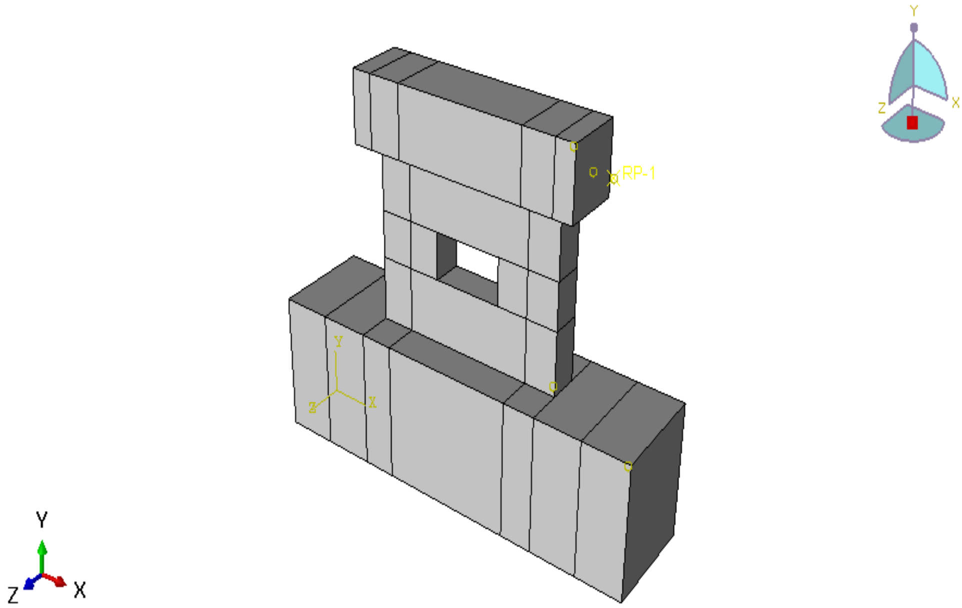

Figure 4.7: RC Shear Wall Model in ABAQUS Software with one Rectangular Opening.

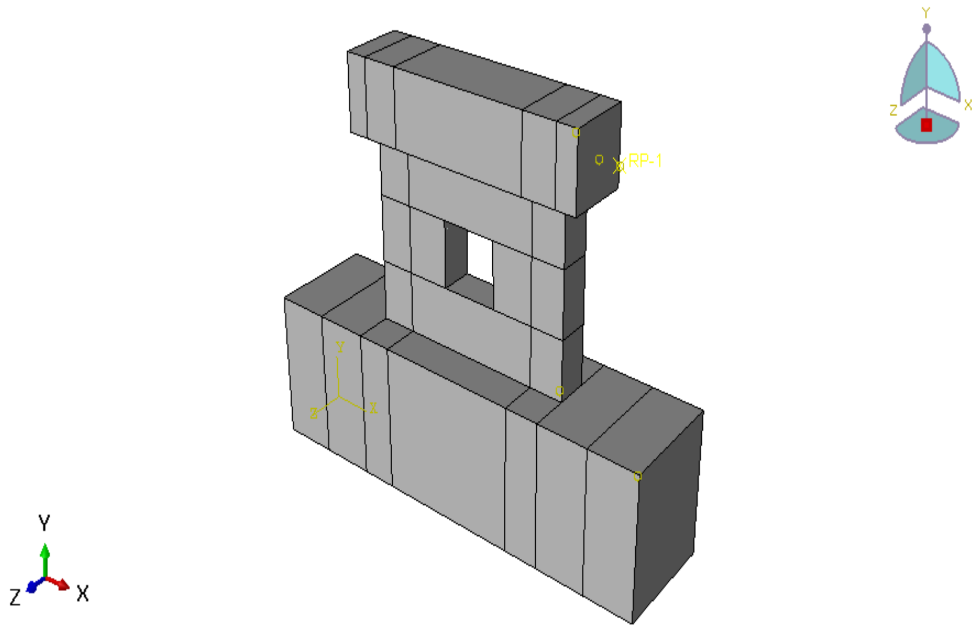

Figure 4.8: RC Shear Wall Model in ABAQUS Software with one Square Opening.

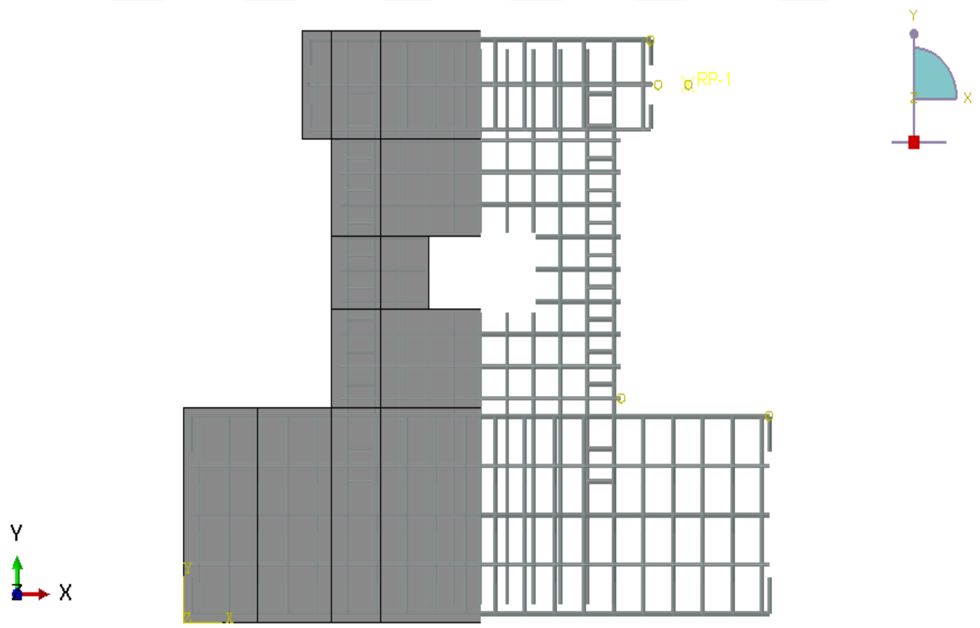

Figure 4.9: RC Shear Wall Model in ABAQUS Software with one Rectangular Opening in 2d Dimension (a).

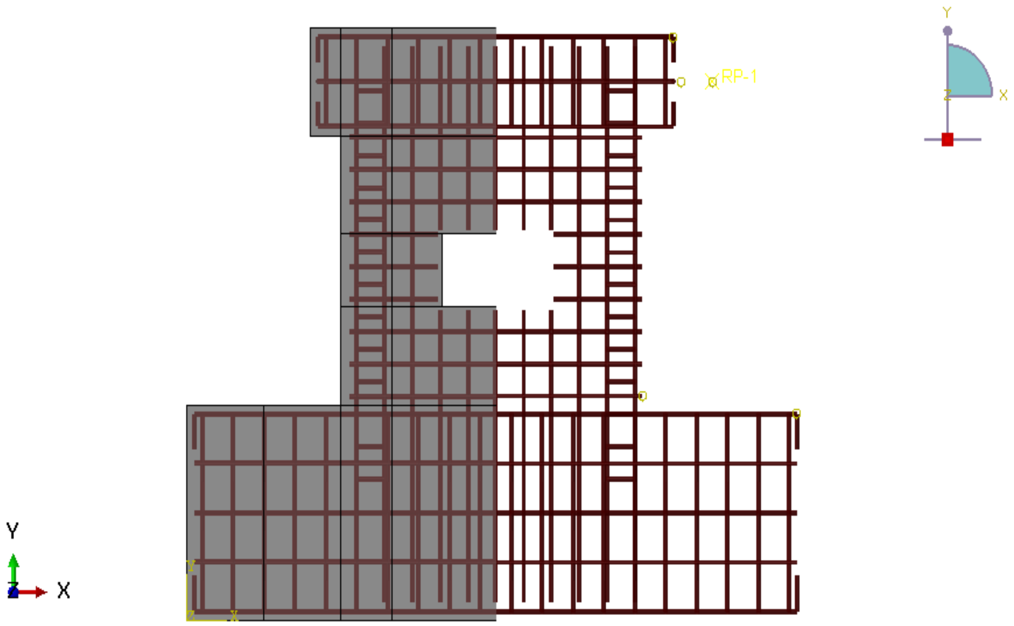

Figure 4.10: RC Shear Wall Model in ABAQUS Software with one Rectangular Opening in 2d Dimension (b).

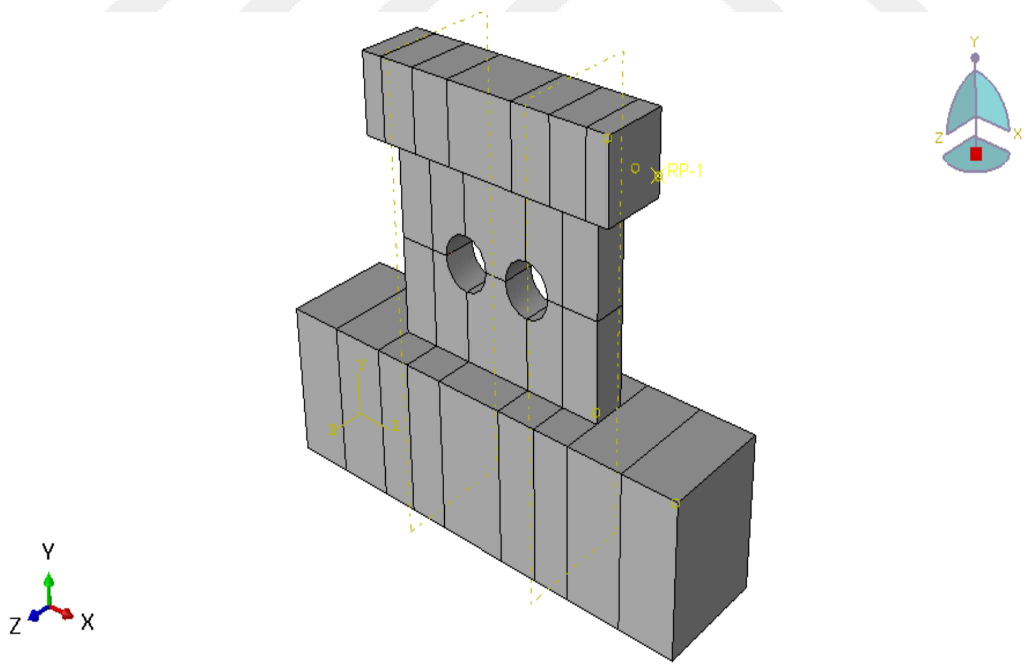

Figure 4.11: RC Shear Wall Model in ABAQUS Software with two Circular Openings.

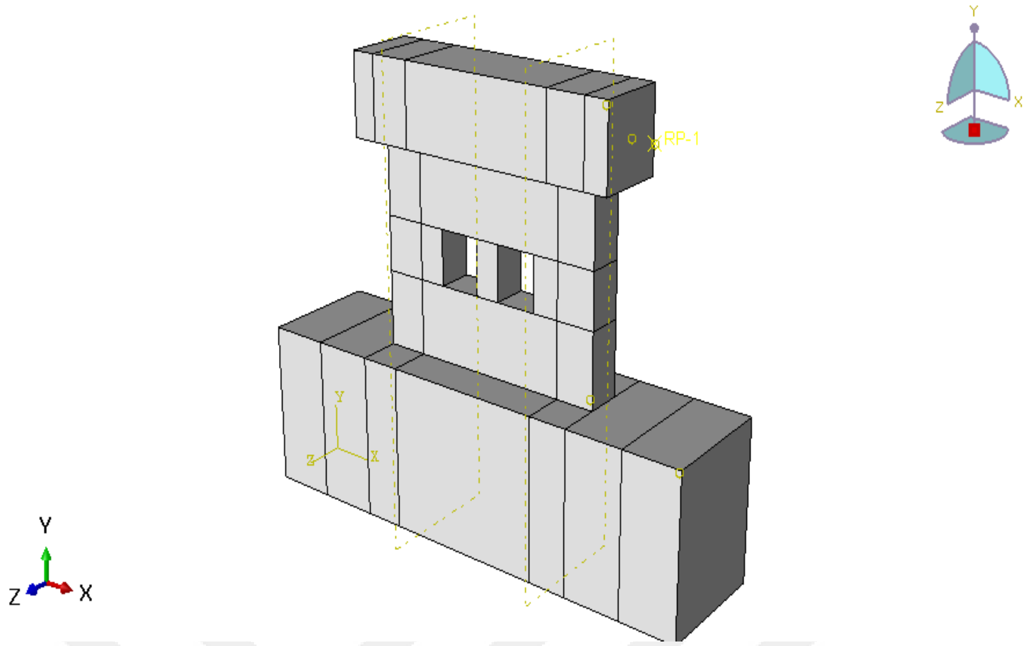

Figure 4.12: RC Shear Wall Model in ABAQUS Software with Two Square Openings.

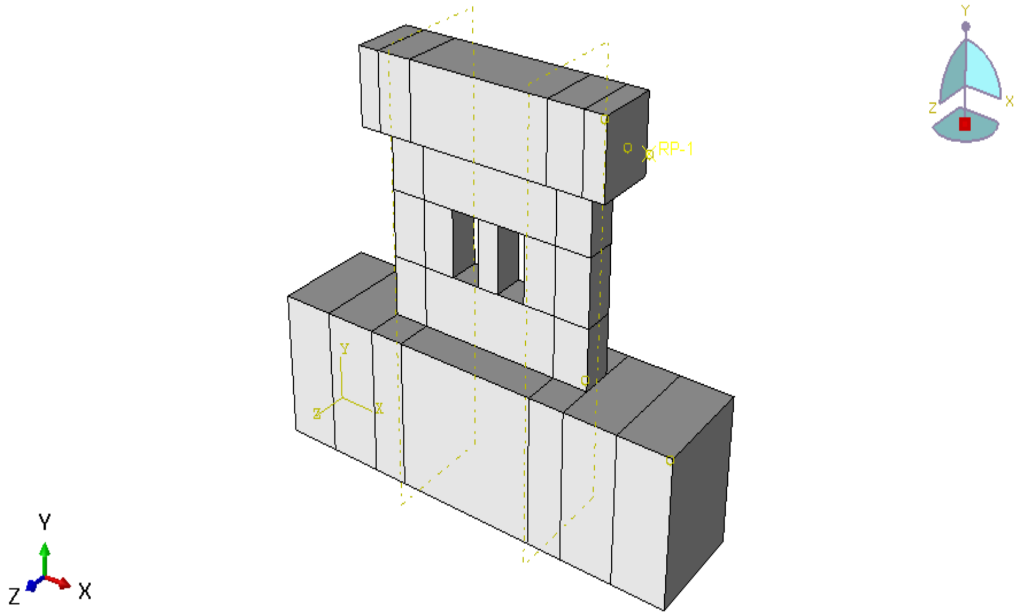

Figure 4.13: RC Shear Wall Model in ABAQUS Software with two Rectangular Openings.

4.3 NUMERICAL LOADS DEFLECTIONS RESPONSE CURVES

Figure (4.1) to (4.12) Show how the results of the experimental testing differ from the load-midspan deflection response relationship obtained by the FE analysis. The findings of the actual testing almost exactly match the behaviour that the FE analysis predicted. The ABAQUS computer method projected an ultimate load capacity that was, on average, 1.2% higher than the experimental ultimate load capacity that was recorded. The deflection at ultimate loads varied on average by 1.3% between experimental and numerical values, although this difference was not statistically significant. This indicates that the failure processes of the reinforced concrete beams have been faithfully modelled by the constitutive models.

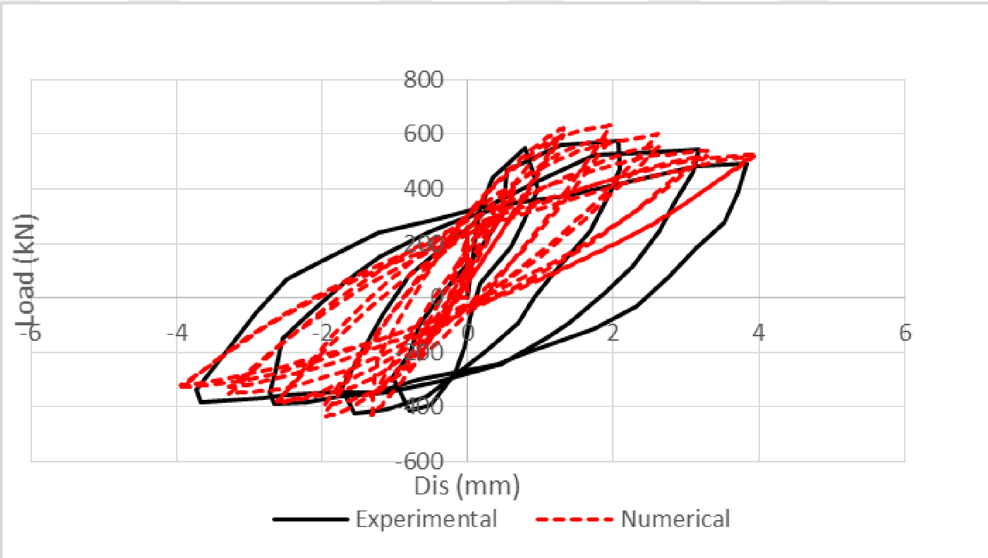

Figure 4.14: W15 Validation Load Displacement Curve Obtained from Experimental Test and Numerical Analysis.

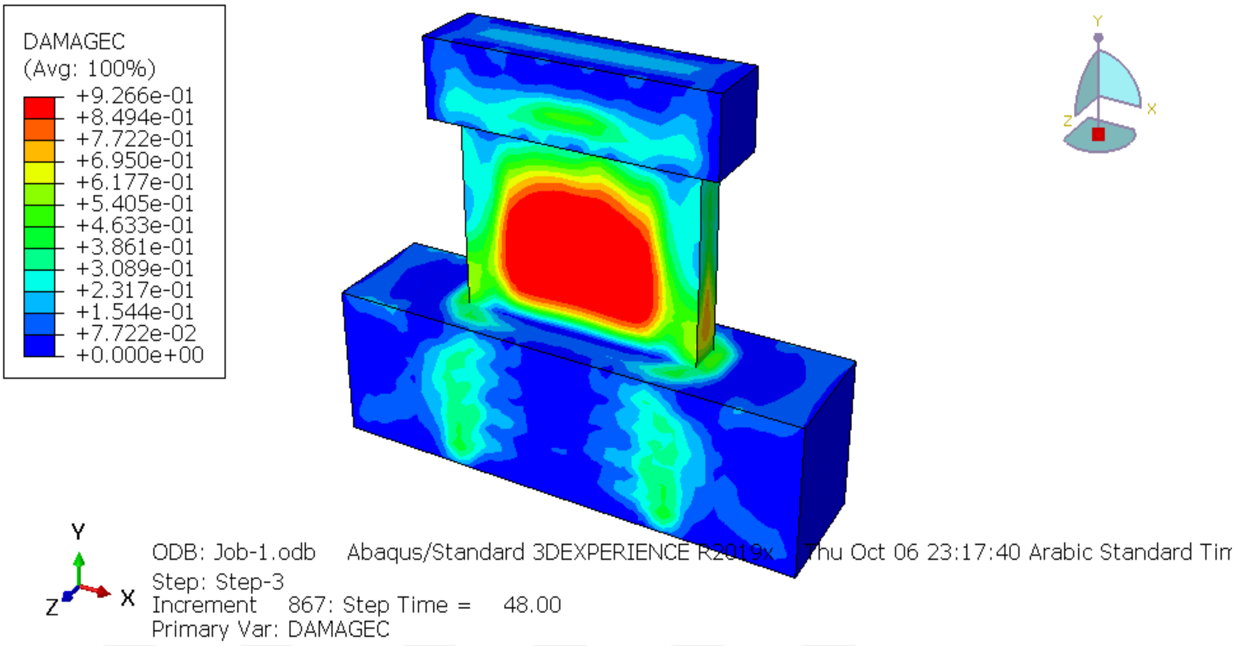

Figure 4.15: Numerical Load Deflection Responses of The Simulate RC Shear Wall.

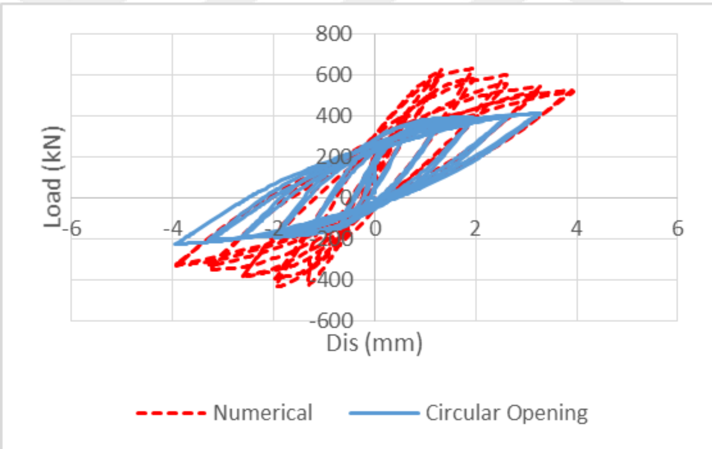

Figure 4.16: Simulated Model with one Circular Opening Load Displacement Curve.

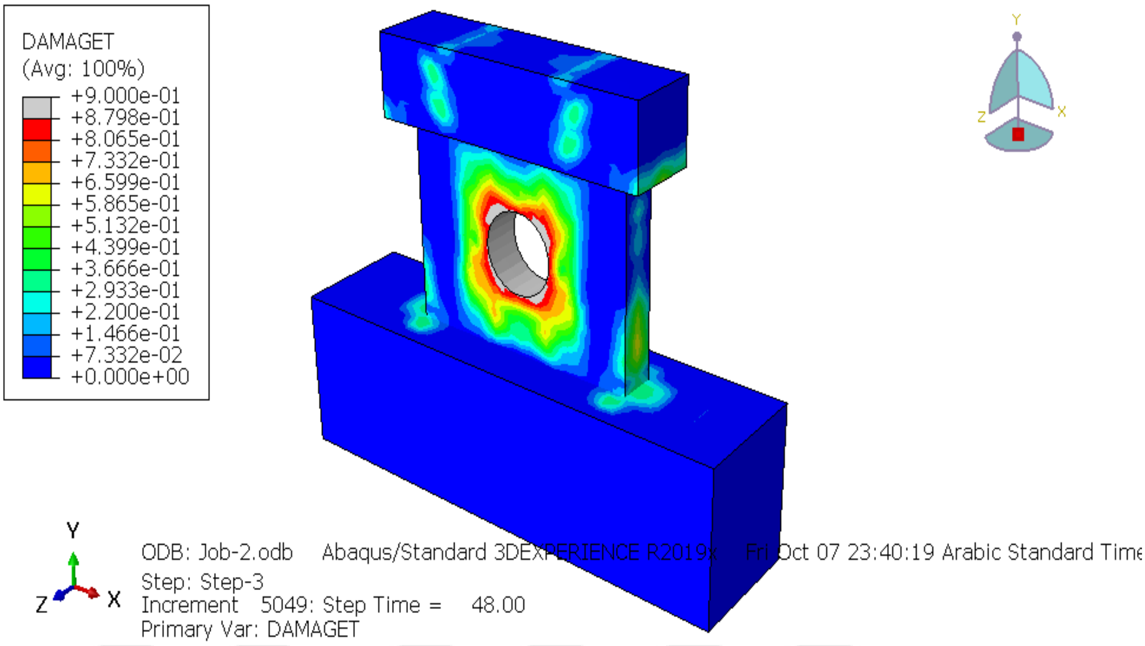

Figure 4.17: Numerical Load Deflection Responses of The Simulate RC Shear Wall with one Circular Opening.

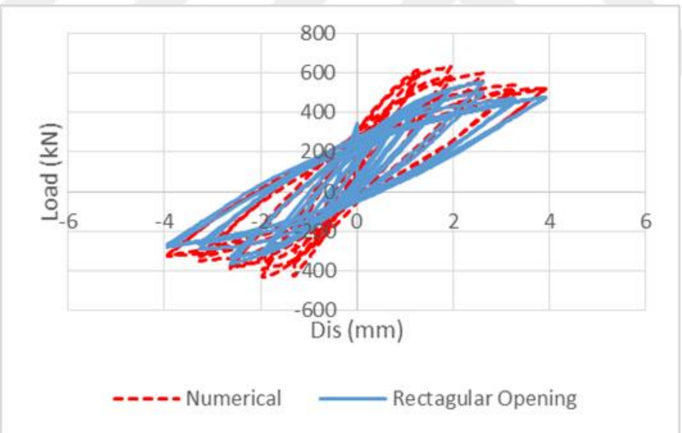

Figure 4.18: Simulated Model with One Rectangular Opening Load Displacement Curve.

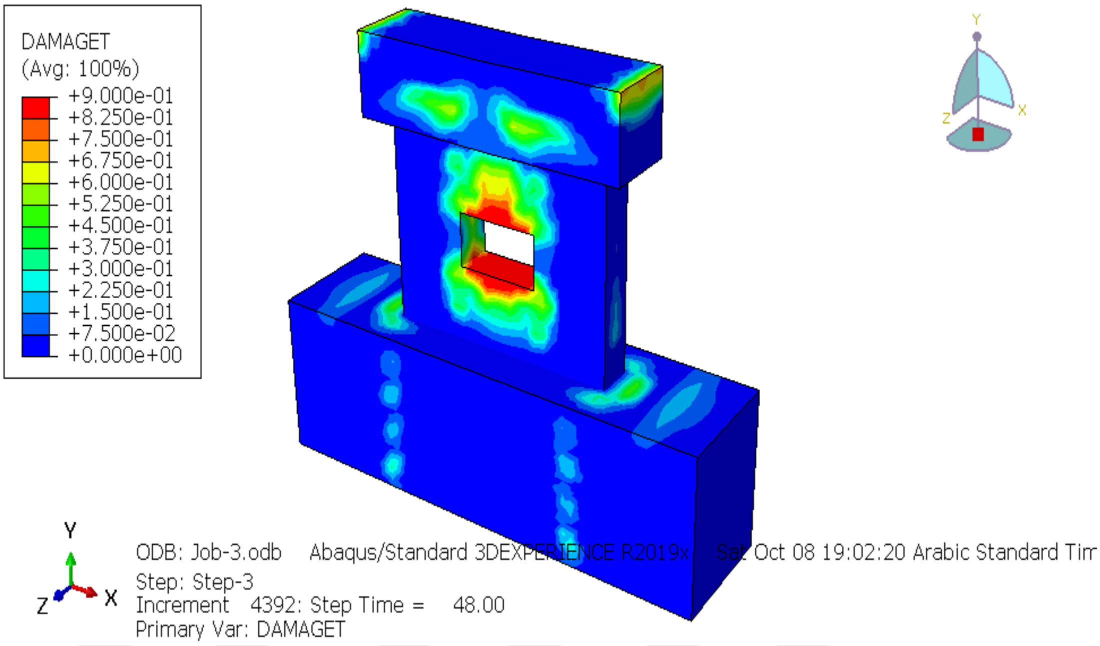

Figure 4.19: Numerical Load Deflection Responses of The Simulate RC Shear Wall with one Rectangular Opening.

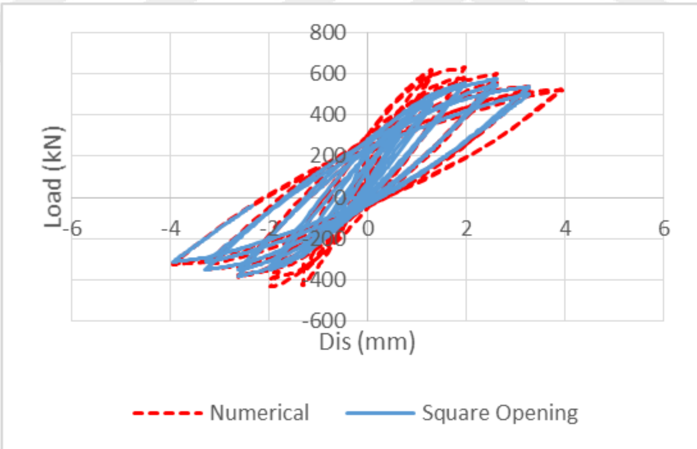

Figure 4.20: Simulated Model with One Square Opening Load Displacement Curve.

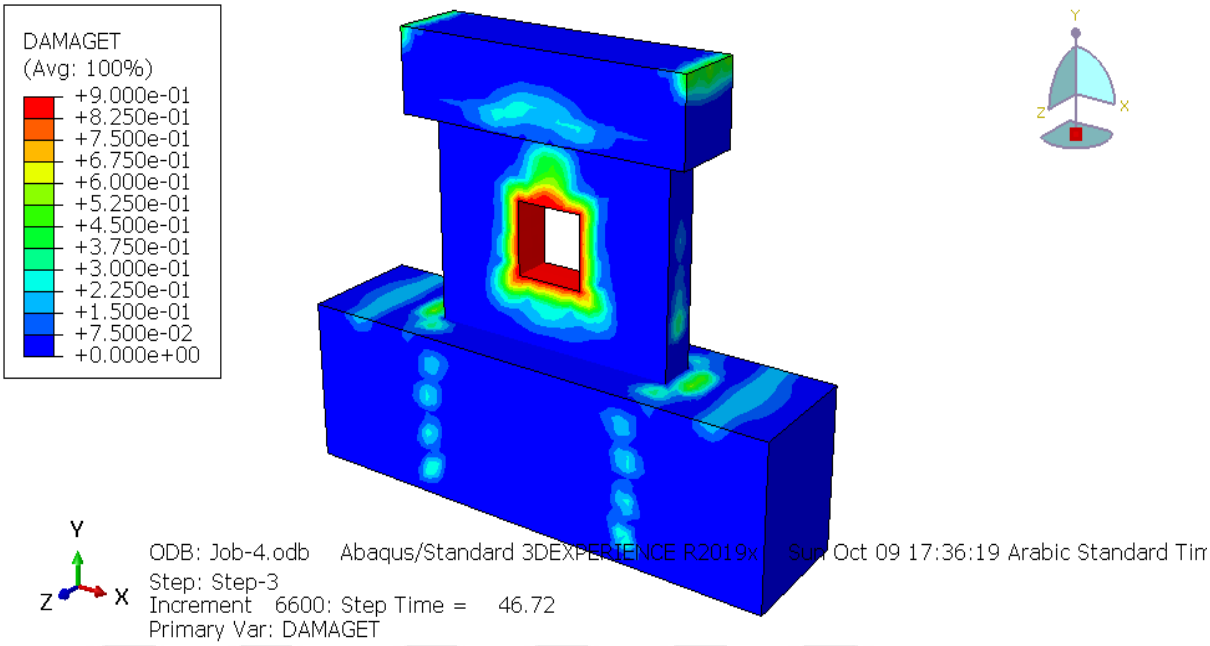

Figure 4.21: Numerical Load Deflection Responses of The Simulate RC Shear Wall with one Square Opening.

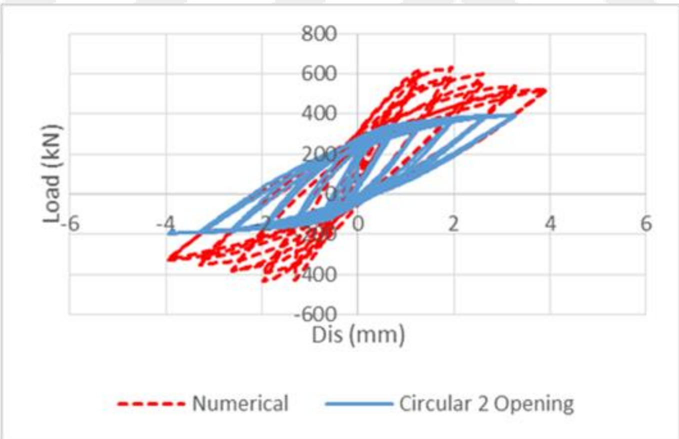

Figure 4.22: Simulated Model with two Circular Openings Load Displacement Curve.

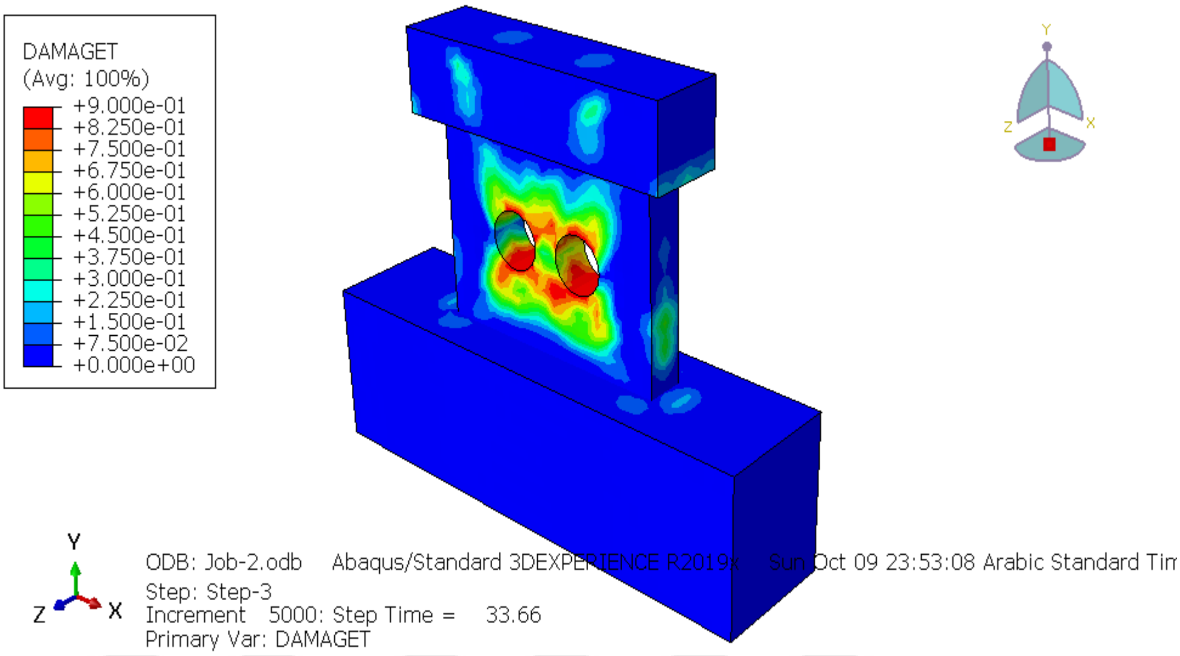

Figure 4.23: Numerical Load Deflection Responses of The Simulate RC Shear Wall with two Circular Openings.

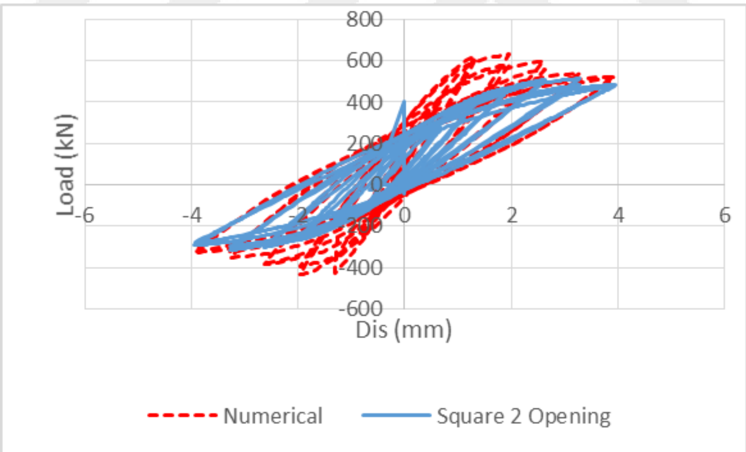

Figure 4.24: Simulated Model with two Square Openings Load Displacement Curve.

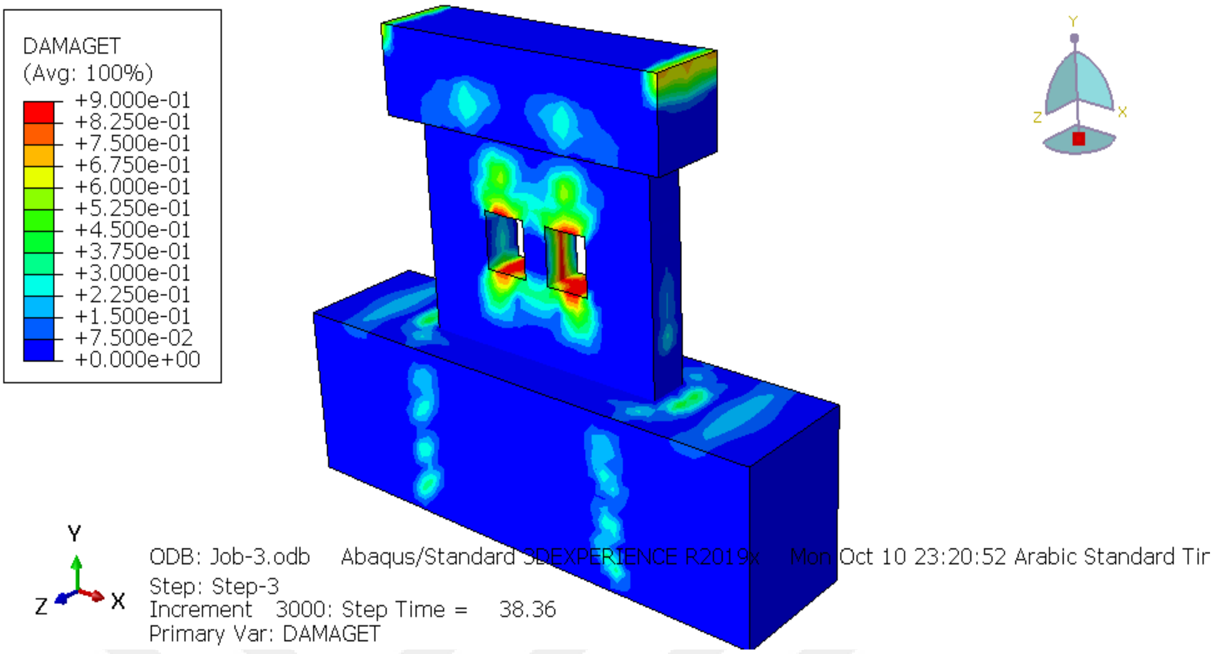

Figure 4.25: Numerical Load Deflection Responses of The Simulate RC Shear Wall with two square Openings.

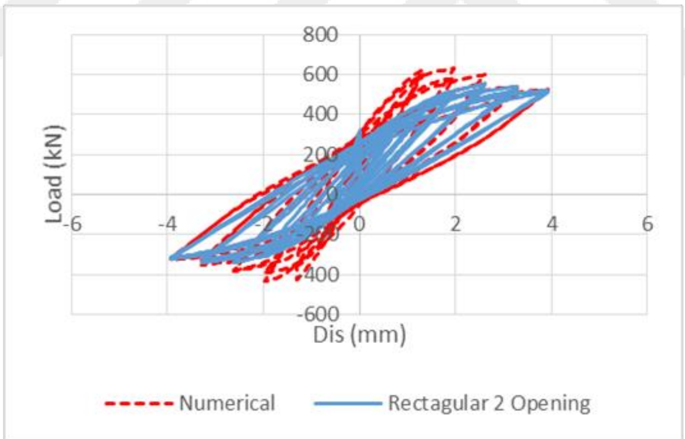

Figure 4.26: Simulated Model with two Rectangular Openings Load Displacement Curve.

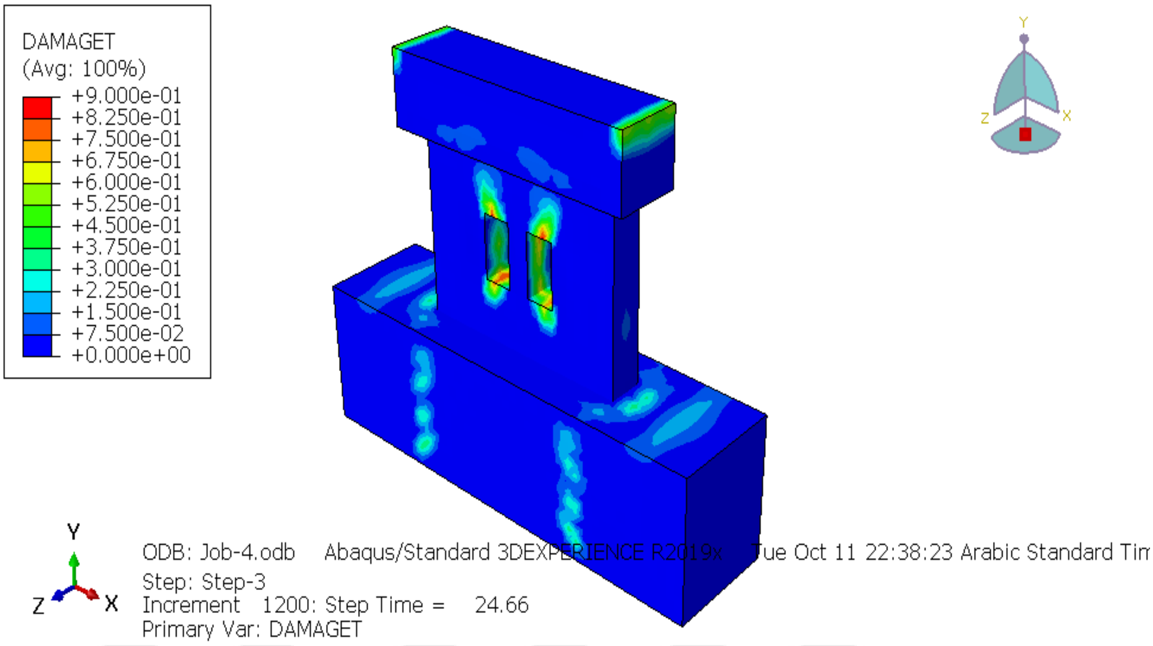

Figure 4.27: Numerical Load Deflection Responses of The Simulate RC Shear Wall with two Rectangular Openings.

By examining the load displacement diagram in the figures above, the following results is obtained:

Table 4.2: Load Displacement.

Model	Max. displacement	Load @ max. dis.
Reference model	3.921	524.67
Model with one circular opening	3.47	407.815
Model with one rectangular opening	3.920	473.743
Model with one square opening	3.263	502.708
Model with two circular openings	3.258	389.938
Model with two rectangular openings	3.913	511.655
Model with two square openings	3.935	477.707

5. CONCLUSION AND FUTURE WORKS

5.1 CONCLUSION

Based on the comprehensive results of the finite-element analysis, the following are the most important findings:

The model with two rectangular apertures that is subjected to the same impact of loads and displacement is the most ductile and exhibits a harderening behaviour than the other models.

According to the finite element results, the ductility of the simulated model with two rectangular apertures is equivalent to 98% of the ductility of the reference model.

According to the finite element results, the weakest simulated model under the identical stress conditions is the model with two circular apertures, whose ductility is 74% of the ductility of the reference model.

Comparing the data, the model with a single square aperture exhibits the best behaviour under a peak load effect resistance of 577.752; although this model failed before reaching the maximum displacement, it was able to reach the maximum resistance among the other models.

The results indicate that the shape and size of the opening have a substantial effect on the ductility of RC shear walls. Hence, when it is introduced in the design of the shear wall for architectural purposes, the lack of ductility must be understood in terms of its shape, size, and distribution, as well as how to lessen or treat it.

5.2 FUTURE WORKS

a. The effects of cracking and maximum shear strengths in a diagonally reinforced concrete skinny beam are explored experimentally as well as conceptually. The focus of this investigation is on the roles that tensile steel reinforcement, concrete compression strength, and beam size play in the process.

b. Experimentation and analysis are being used to investigate the question of whether or not the size of the beam has an effect on the ultimate cracking and shear strengths of cross-wise continuous concrete reinforced deep beams.

c. Examining, both experimentally and conceptually, the effect that beam size has on cracking and ultimate shear strengths in shear and non-shear reinforced concrete skinny beams, with the beam width held constant.

d. The formulas of the British, American, European, and Canadian codes for shear and non-shear reinforced concrete beams are analyzed in order to gain a better understanding of how the size of the beam affects the capacity of the concrete.

e. The empirical formula that was proposed as well as any extra formulas that were developed by the researchers are utilized in order to make a comparison between concrete beams equipped with and without stirrups with regard to their shear capacity.

REFERENCES

[1]. Arthi, H. T., and Kumar, S. G., (2015). Behavior of R.C Shear Wall with Staggered Openings under Seismic Loads. International Journal for Research in Emerging Science and Technology. Vol.2, Issue 3.

[2]. Abo El-saad, M., and Salama, M., (2015). Estimation of Period of Vibration for Concrete Shear Wall Buildings. Housing and Building National Research Center Journal. Vol.13, Issue 3.

[3]. ACI 318 2014. Building Code Requirements for Structural Concrete (ACI 318M-14): an ACI standard: Commentary on building code requirement for structural concrete (ACI 318M-14), Farmington Hills, MI, American Concrete Institute.

[4]. Aghayari, R., Ashrafy, M., and Roudsari, M., (2017). Estimation of the Base Shear and Fundamental Period of Low-Rise Reinforced Concrete Coupled Shear Wall Structures. Asian Journal of Civil Engineering Vol.18, Issue 7.

[5]. Ambrose, J., and Vergun, D., (1995). Simplified Building Design for Wind and Earthquake Forces. Third Edition, John Willey & Sons INC.

[6]. ASCE 2016. Minimum design loads for buildings and other structures, Reston, Va., American Society of Civil Engineers: Structural Engineering Institute.

[7]. Balkaya, C., and Kalkan, E., (2003). Estimation of Fundamental Period of Shear-Wall Dominate Building Structures. The Journal of Earthquake Engineering and Structural Dynamics, Vol.32, Issue 7.

[8]. Bishop, R. E., Johnson, D. C., 1979: The Mechanics of Vibration, Cambridge University Press.

[9]. Brandow, G. E., and Virdee, A., (1995). Design of Reinforced Masonry Structures. Fifth Edition, Concrete Masonry Association of California and Nevada,CA.

[10]. BUNGALE, S. T., 2010. Reinforced Concrete Design of Tall Buildings, CRC Press Taylor & Francis Group.

[11]. Chalah, F., Rezgui, L., Falek, K., Djellab, S., and Bilal, A., (2014). Fundamental Vibration Period of SW Buildings. APCBEE Procedia, Vol.9.

[12]. CSI, C. A. S., INC., Berkeley, California, USA 2017. SAP2000

[13]. V.20.0.0, Integrated Finite Element Analysis and Design of Structures.

[14]. Goel, K. R. and Chopra, A. K. (1998). Period Formula for Concrete Shear Wall Buildings. ASCE Journal of Structural Engineering, Vol.124, Issue 4.

[15]. Hsiao, K. J., (2014). Hand- Calculated Procedure for Rigidity Computation of Shear Walls With Openings. ASCE Journal of Structural Engineering, Vol.19, Issue 4.

[16]. J'aidi, Y. T., (2002). Rigidity of Reinforced Concrete Shear Walls and Effect of Openings. Master thesis. An-Najah National University.

[17]. Jordanian code for loads and forces. Amman, Jordan, Building Research Center for Ministry of Public Works & Housing, 2006.

[18]. Kwon, O. H., and Kim, E., (2010). Evaluation of Building Period Formulas for Seismic Design. The structural design of tall and special building journal, Vol.39, Issue14.

[19]. Lee, L. H., Chang, K. K., and Chun, Y., (2000). Experimental Formula for the Fundamental Period of RC Buildings With Shear- Wall Dominate System. The structural design of tall and special building journal, Vol.7. Issue 4.

[20]. Neuenhofer, A., (2006). Lateral Stiffness of Shear Walls With Openings. ASCE Journal of Structural Engineering, Vol.132, Issue 11.

[21]. Nyarko, H. M., Draganic, H., Moric, D., Stefic, T., (2015). Comparison of Fundamental Period of Reinforced Shear Wall Dominate Building Models with Empirical Expressions. Technical Gazette Journal. Vol.22, Issue 3.

[22]. Sozen, M. A. (1989). Earthquake response of buildings with robust walls. Fifth Chilean Conference on Seismology and Earthquake Engineering, Santiago, Chile.

[23]. Wallace, W. J., and Moehle, P. J., (1992). Ductility and Detailing Requirements of Bearing Wall Buildings. ASCE Journal of Structural Engineering, Vol.118, Issue 6.

[24]. N. A. Suparlan, M. A. Ku Ayob, H. Ahmad, S. H. Hamzah, and M. H. Mohd Hashim, “Preliminary investigation on the flexural behaviour of steel fibre reinforced self-compacting concrete ribbed slab,” Sci. Res. J., vol. 15, no. 1, pp. 32–45, 2018.

[25]. U. Obinna, “Structural Design of Ribbed Slabs.” 2020. [Online]. Available: https://structville.com/2020/03/structural-design-of-ribbed-slabs.html

[26]. American Society of Civil Engineers, “ASCE 7 standard | ASCE.” 2022. [Online]. Available: https://www.asce.org/publications-and-news/asce-7

[27]. N. Nassif, W. Zeiada, G. Al-Khateeb, S. Haridy, S. Altoubat, “Assessment of Punching Shear Strength of Fiber-reinforced Concrete Flat Slabs Using Factorial Design of Experiments,” Jordan J. Civ. Eng., vol. 16, no. 1, pp. 139–154, 2022.

[28]. E. Tekleab , T. Wondimu, “Behavior of Steel-Fiber-Reinforced Concrete (SFRC) Slab-on-Grade under Impact Loading,” Adv. Civ. Eng., vol. 2022, 2022.

[29]. ACI committee 318, Building Code Requirements for Structural Concrete and Commentary (ACI 318M-11). 2011.

[30]. D. Ajema, A. Abeyo, “Cost Comparison between Frames with Solid Slab and Ribbed Slab using HCB under Seismic Loading,” Int. Res. J. Eng. Technol., vol. 9001, no. 1, pp. 109–116, 2008.

[31]. Y. A. Alvarado, B. Torres, M. Buitrago, D. M. Ruiz, S. Y. Torres, R. A. Alvarez, “Dynamic punching shear tests of flat slab-column joints with 5D steel fibers,” Struct. Eng. Mech., vol. 81, no. 3, pp. 281–292, 2022.

[32]. N. F. Zamri, R. N. Mohamed, D. Awalluddin, R. Abdullah, “Experimental evaluation on punching shear resistance of steel fibre reinforced self-compacting concrete flat slabs,” J. Build. Eng., vol. 52, 2022.

[33]. D. Xiang, S. Liu, Y. Li, Y. Liu, “Improvement of flexural and cyclic performance of bridge deck slabs by utilizing steel fiber reinforced concrete (SFRC),” Constr. Build. Mater., vol. 329, 2022.

[34]. N. A. Suparlan, M. A. Ku Ayob, H. Ahmad, S. H. Hamzah, and M. H. Mohd Hashim, “Preliminary investigation on the flexural behaviour of steel fibre reinforced self-compacting concrete ribbed slab,” Sci. Res. J., vol. 15, no. 1, pp. 32–45, 2018.

[35]. N. Altay Eren, “Punching shear behaviour of geopolymer concrete two-way flat slabs incorporating a combination of nano silica and steel fibers,” Constr. Build. Mater., vol. 346, 2022.

[36]. L. Nguyen-Minh, M. RovňÁk, T. Tran-Quoc, K. Nguyen-Kim, “Punching shear resistance of steel fiber reinforced concrete flat slabs,” Procedia Eng., vol. 14, pp. 1830–1837, 2011.

[37]. M. Saadoon, M. A. Mashrei, K. A. Al Oumari, “Punching shear strength of recycled aggregate-steel fibrous concrete slabs with and without strengthening,” Adv. Struct. Eng., vol. 25, no. 10, pp. 2175–2190, 2022.

[38]. Jahami, Y. Temsah, J. Khatib, M. Sonebi, “Rehabilitation of reinforced concrete slabs damaged by impact loading using swimmers as shear reinforcement,” Mater. Today Proc., vol. 58, pp. 1251–1257, 2022.

[39]. S. Sahoo , B. Singh, “Steel Fiber Reinforced Recycled Aggregate Concrete Slab Punching Shear Capacity,” Mag. Concr. Res., vol. 74, pp. 1–42, 2022.

[40]. G. Velayutham , C. B. Cheah, “The effects of steel fibre on the mechanical strength and durability of steel fibre reinforced high strength concrete (SFRHSC) subjected to normal and hygrothermal curing,” MATEC Web Conf., vol. 10, 2014.

[41]. Z. Ghuraibaw, S. Naimi, “Modeling and Designing Concrete With Steel Fibers to Improve Multiple-Ribbed Slabs”, International Journal on “Technical and Physical Problems of Engineering” (IJTPE), Issue 54, Volume 15, Number 1, pages 309-317, March 2023

[42]. H.A. Alobadi, S. Naimi, “A Study of Construction Delays”, International Journal on “Technical and Physical Problems of Engineering” (IJTPE), Issue 54, Volume 15, Number 1, pages 296-308, March 2023

[43]. S. Mahal, S. Naimi, “Impact of Project Management on Success Criteria”, International Journal on “Technical and Physical Problems of Engineering” (IJTPE), Issue 54, Volume 15, Number 1, pages 318-326, March 2023.

[44]. T. Shaker, S. Naimi, “Productivity in Constructions with Role of Site Effect and Complexity Variables”, International Journal on “Technical and Physical Problems of Engineering” (IJTPE), Issue 54, Volume 15, Number 1, Page 327-333, March 2023.

[45]. Sepanta Naimi, Önder Peker, “Deprem Etkileri Altındaki Farklı Tiplerde Çelik Yapıların StaSTEEL ve SAP2000 Kullanılarak Karşılaştırılması”, Journal of the Institute of Science and Technology, Vol. 12, Issue 3, PP. 1577-1591, 2022.

[46]. Yalda Dehqan Nezhad, Sepanta Naimi, “Numerical investigation of precast reinforced concrete beam–to–column joints by replaceable damper”, Journal of Sustainable Construction Materials and Technologies, Vol. 7, Issue 2, PP. 81 – 87, 2022.

[47]. Sepanta Naimi, Mohammad Ali Karimi, “Pavement Management System Investigation in Case of Afghanistan”, Cumhuriyet Science Journal, Vol. 40, Issue 1, pages 221-232 , 2019. doi: 10.17776/csj.471334.

[48]. Taha Vardar, Mehmet Fatih Altan, Sepanta Naimi, “Economic and Technological Evaluation of Transportation System, New Trends”, Journal of Sustainable Construction Materials and Technologies, pages 83-88, 2017.

[49]. Layth AL Musawi, Sepanta Naimi, “The management of construction projects in Iraq and the most important reasons for the delay”, Acta Logistica, Vol. 10, Issue 1, Page 61-70, 2023.

[50]. Ali Raad Mohammed, Sepanta Naimi, “The Effectiveness of Thermal Insulation of the Exterior Composite Walls of Buildings in Iraq Based on Different Materials and Climate Regions using Engineering Applications”, International Journal of Intelligent Systems and Applications in Engineering, Vol. 11, Issue 4s, Page 594-601, 2023.